

MODELING STUDY OF COUPLING EXOTHERMIC AND ENDOTHERMIC
REACTIONS IN A SINGLE REACTOR DESIGN – A CASE STUDY USING
OXIDATIVE COUPLING OF METHANE AND METHANE
DEHYDROAROMATIZATION

A Thesis

by

MUHAMMAD UMAR JAMIL

Submitted to the Graduate and Professional School of
Texas A&M University
in partial fulfillment of the requirements for the degree of

MASTER OF SCIENCE

Chair of Committee, Patrick Linke
Co-Chair of Committee, Ma'moun Al-Rawashdeh
Committee Members, Othmane Bouhali

Head of Department, Patrick Linke

August 2021

Major Subject: Chemical Engineering

Copyright 2021 Muhammad Umar Jamil

ABSTRACT

Around 3 billion tons of carbon dioxide is emitted every year through the chemical and petrochemical industries. To reduce these emissions and utilize the natural resources better, new sustainable routes are needed to replace the highly optimized and cost-competitive methane conversion to chemicals via the indirect syngas route. Of the proposed directed routes are the oxidative and non-oxidative coupling of methane, which have not yet been commercialized. Among other challenges, these routes require high operating temperatures (600 – 1000 °C) and strict heat management. An idea to address these challenges is to consider both chemistry routes in the same chemical plant as this can have many potential advantages. One of these potential advantages is reaching autothermal operation which reduces the energy demands and carbon emissions. This work aims to explore options for thermal coupling of exothermic and endothermic reactions in a single reactor but without any mass integration. The first reaction is the oxidative coupling of methane (OCM) which is highly exothermic ($\Delta H^{\circ}_{\text{rxn}} = -141$ kJ/mol.CH₄) and produces C₂+ products like ethane and ethylene. The second reaction is methane dehydroaromatization (MDA) which is endothermic ($\Delta H^{\circ}_{\text{rxn}} = +88.4$ kJ/mol.CH₄) and yields C₆+ products like benzene, toluene, and naphthalene.

Available kinetic models for OCM and MDA are studied from the literature and an separate ideal packed bed reactor was modeled using relatively simple kinetics. Multiple optimization studies via single-variable-at-a-time were performed and an operating window for thermal coupling is identified in between 700 – 850 °C temperature, 1 – 5 atm pressure, GHSV 830 – 14,000 h⁻¹, and heat duties of 1–13 MW. Owing to many input and

output variables, several design options can be proposed. Therefore, we developed a methodology with visual representation to help navigate between different optimization options for thermal coupling. A study was carried out by having each reaction in a separate reaction channel divided by a channel wall using heat transfer and pressure drop correlations from literature assess the temperature profile. As a starting point, both reaction channels are considered straight, having identical channel length, and filled with spherical catalyst particles in an ideal packed bed reactor. Parameters affecting such a reactor design were studied, which include heat transfer coefficient, diluents, catalyst profiling and flow direction. Using the proposed methodology, further work can mainly be carried out for achieving a global optimum via multi-objective optimization. This would allow for quick decision making between different kinetic models and reactor designs with the given targets and constraints.

DEDICATION

I dedicate this thesis to mummy, daddy and my brothers for their love, patience, and support.

ACKNOWLEDGEMENTS

First and foremost, I would like to offer this endeavor to Almighty Allah for blessing me with the strength, the wisdom, and good health that enabled me to complete this research.

I would like to express gratitude to my mentor and advisor, Dr. Ma'moun Al-Rawashdeh, who guided me through his invaluable advises and in-depth knowledge. He not only directed me towards the important aspects of this multi-disciplinary research topic but also developed my professional skills. I am also appreciative of my committee members, Dr. Patrick Linke and Dr. Othmane Bouhali, for their guidance and assistance throughout the course of this research. Moreover, I would like to acknowledge the Total research team for their valuable guidance.

Beyond the scope of this research, I really appreciate the opportunities of professional development that Ms. Lana El-Ladki has provided through Center for Teaching and Learning. I would also like to thank Ms. Hania Ayyash for her administrative support which enabled me to be a part of this prestigious institution.

Furthermore, I would like to express my deepest gratitude to my mentor in Pakistan, Mr. Inamullah Khan, whose motivation and support pushed me to develop myself further in the field of engineering. I am also extremely grateful to my friend, Kashaf Bakali, for her continued support throughout, without which this would have not been possible.

Most importantly, I want to express my deep appreciation to my family, my mother, father, and brothers, for their unconditional love and encouragement.

CONTRIBUTORS AND FUNDING SOURCES

This work was supervised by a thesis committee consisting of Professor Dr. Ma'moun Al-Rawashdeh, Professor Dr. Patrick Linke of the Department of Chemical Engineering and Professor Dr. Othmane Bouhali of the Department of Research Computing.

All the work conducted for the thesis was completed by the student separately.

Funding Sources

This work was made possible by internal funding from Texas A&M University at Qatar, and Total scholarship in the field of sustainable natural gas conversion to chemical products in Qatar.

NOMENCLATURE

$C_{P,i}$	Specific heat capacity of component i (J mol ⁻¹ K ⁻¹)
$\Delta C_{P,j,i}$	Delta specific heat capacity for reaction j with respect to component i (J mol ⁻¹ K ⁻¹)
d_t	Tube diameter (cm)
d_p	Particle diameter (cm)
F_i	Molar flowrate of component i (mol h ⁻¹)
$H_{f,i}$	Enthalpy of formation of component i (J mol ⁻¹)
$\Delta H_{j,i}$	Delta enthalpy of reaction j at temperature T (J mol ⁻¹)
$\Delta H_{j,i}^{\circ}$	Standard delta enthalpy of reaction j at temperature T_R (J mol ⁻¹)
k_j	Reaction rate constant (mol, atm, s, cm ³)
k_{fj}	Forward rate constant of reaction j (mol, atm, h, g cat)
K_{pj}	Equilibrium constant of reaction j (atm)
m_a	Molar flowrate of the coolant (mol h ⁻¹)
p_i	Partial pressure of component i (atm)
$Q_{g,n}$	Heat generated or required by reactions taking place in compartment n (J cm ⁻¹ h ⁻¹)
Q_{ex}	Heat removed from the compartment (J cm ⁻¹ h ⁻¹)
$r_{j,i}$	Rate of formation of component i in reaction j (mol cm ⁻³ s ⁻¹)
$r_{i,net}$	Net reaction rate for component i, equal to sum of rates of all reactions q, in which i appears, $r_{i,net} = \sum_j^q r_{j,i}$
R	Ideal gas constant

R_n	Resistance to heat transfer in compartment n
T_n	Process side temperature of compartment n (K)
T_R	Reference temperature, 298.15 (K)
U_{overall}	Overall heat transfer coefficient (J cm ⁻³ s ⁻¹ K ⁻¹)
V_{reactor}	Reactor volume (cm ³)
V_{gas}	Gas volume (cm ³)
V_{catalyst}	Catalyst volume (cm ³)
V_{diluent}	Diluent volume (cm ³)
A_h	Heat exchanging surface, OCM side (cm ²)
A_c	Heat exchanging surface, MDA side (cm ²)
A_m	Log mean of A_h and A_c (cm ²)
Δw	Thickness of the dividing wall (cm)
Δr	Radius of the MDA packed bed (cm)
r_h	Inner tube radius of the OCM compartment (cm)
r_w	Outer tube radius of the OCM compartment (cm)
n	Compartment of coupled reactor (h: OCM, c: MDA)
Re	Reynold's number, $Re = \frac{\rho v d_p}{\mu}$
Pr	Prandtl number, $Pr = \frac{c_p \mu}{k}$
Nu	Nusselt's number, $Nu = h_w \frac{d_p}{k}$
d_p	Catalyst particle diameter (cm)
v	Volumetric flowrate of the gas (cm ³ s ⁻¹)

k Thermal conductivity of the gas ($W\ cm^{-1}\ K^{-1}$)

Greek letters:

η_j Approach to equilibrium

θ_a Stoichiometric reaction coefficient of reference component a

θ_i Stoichiometric reaction coefficient of component i

$\rho_{,gas}$ Gas density ($g\ cm^{-3}$)

$\rho_{,bulk}$ Bulk density ($g\ cm^{-3}$)

$\varepsilon_{,gas}$ Gas void fraction

$\varepsilon_{,catalyst}$ Catalyst void fraction

$\varepsilon_{,diluent}$ Diluent void fraction

λ_w Thermal conductivity of dividing wall ($W\ cm^{-1}\ K^{-1}$)

μ Gas viscosity ($cm^2\ s^{-1}$)

α_n Heat transfer coefficient for compartment n ($kcal\ m^{-2}\ h^{-1}\ K^{-1}$)

$\alpha_{w,n}$ Wall heat transfer coefficient for compartment n ($kcal\ m^{-2}h^{-1}\ K^{-1}$)

$\alpha_{bed,n}$ Overall effective conductivity of compartment n ($kcal\ m^{-2}h^{-1}\ K^{-1}$)

$\alpha_{w,n}^o$ Static contribution to $\alpha_{w,n}$ ($kcal\ m^{-2}\ h^{-1}\ K^{-1}$)

$\alpha_{w,n}^o$ Static contribution to $\alpha_{w,n}$ ($kcal\ m^{-2}\ h^{-1}\ K^{-1}$)

TABLE OF CONTENTS

	Page
ABSTRACT	II
DEDICATION	IV
ACKNOWLEDGEMENTS	V
CONTRIBUTORS AND FUNDING SOURCES.....	VI
NOMENCLATURE.....	VII
TABLE OF CONTENTS	X
LIST OF FIGURES.....	XII
LIST OF TABLES	XV
CHAPTER I INTRODUCTION	16
Motivation	16
Research objectives	21
Research plan	22
CHAPTER II LITERATURE REVIEW	23
General overview	23
OCM kinetic models	24
MDA kinetic models	26
A matrix for selection of kinetic models to be used in this work	27
OCM kinetic model	27
MDA kinetic model.....	29
Kinetic models validation.....	31
CHAPTER III MATHEMATICAL MODELING OF SEPARATE 1-D PSEUDO HOMOGENOUS IDEAL PACKED BED REACTOR MODELS	34
Reactor design equations.....	34
Numerical solution	35
Reactions' parameter calculation	36

CHAPTER IV THERMAL COUPLING OF SEPARATE OCM AND MDA REACTORS	37
Parametric studies of OCM.....	37
Effect of gas hourly space velocity	38
Effect of pressure and temperature.....	39
Effect of feed composition	39
Parametric studies of MDA.....	40
Comparison of OCM and MDA studies.....	41
Reactors coupling using Neural Network diagram	42
A case study using thermal coupling methodology for separate OCM and MDA reactors	44
Defining the case study	44
Solving the case study using the coupling methodology	45
Using of the methodology for other case studies	48
CHAPTER V THERMAL COUPLING OF COUPLED OCM AND MDA REACTORS	50
Reactor design selection, scope and targets	50
Mathematical modeling of coupled 1-D pseudo homogenous single packed bed reactor model.....	51
Reactor design equations.....	52
Selecting acceptable ranges of reactor channels based on non-isobaric analysis of Ergun Equation.....	55
Initial analysis of non-isothermal reactor design based on heat transfer coefficient ...	58
Overall heat transfer coefficient	58
Predicting heat transfer coefficient from correlations in the literature	60
Altering the axial temperature profile to acceptable design targets via catalyst profiling and diluents	65
Effect of diluents on temperature profile	65
Effect of OCM catalyst profiling for a fixed catalyst and diluent void fraction	67
Effect of MDA catalyst profiling for a fixed catalyst and diluent void fraction	69
Co-current versus counter-current flow direction analysis	70
Guidelines for approaching an isothermal reactor temperature and performance	71
Thermal coupling optimization of showcase coupled reactors using neural network ..	72
CHAPTER VI CONCLUSIONS	75
REFERENCES.....	79

LIST OF FIGURES

	Page
Figure I.1 Multiple OCM catalysts reported in the literature [4]	18
Figure I.2 Methane conversion of OCM at multiple operating temperatures [6]	18
Figure I.3 Equilibrium methane conversion of MDA at multiple operating temperatures [7].....	19
Figure I.4 Multiple integration options for OCM and MDA (a) Mass integration option; (b) Process integration option (c) Reactors' heat integration option	21
Figure I.5 Kinetic models of OCM and MDA (a); Two separate reactor models for OCM and MDA (b); OCM-MDA coupled reactor design (c).....	22
Figure I.6 Research flow chart with deliverables.....	22
Figure II.1 (Wang, 1995) Experimental data vs Our simulation.....	32
Figure II.2 (Kao, 1997) Simulation (.) vs Our simulation (-).....	32
Figure II.3 (Zhu, 2018) Simulation vs Our simulation	32
Figure II.4 (Karakaya, 2016) Microkinetic model vs Our simulation	33
Figure III.1 Schematic diagram of separate OCM reactor (left) and MDA reactor (right)	34
Figure III.2 Model flow chart for obtaining the numerical solution	36
Figure IV.1 Concept of Artificial Neural Network diagram with 'n' multiple inputs and outputs.....	43
Figure IV.2 Reactors coupling methodology following similar analogy as ANN.....	44
Figure IV.3 Final results of reactors coupling methodology for the given case study.....	48
Figure IV.4 Multiple thermally coupled case studies for 700, 800 and 850 °C optimized using the proposed methodology	48
Figure V.1 Reactor design from separate reactors to coupled reactors.....	50
Figure V.2 Schematic diagram of thermally coupled OCM-MDA (a) multi-tubular reactor (b) single tube representation (c) elemental segment of one	

reactor channel (d) heat transfer resistances across the radius of reactor	52
Figure V.3 Pressure drop per length for multiple pressure drops per length	56
Figure V.4 Reactor length for multiple space times shown for $dp/dz = 0.05 P_0 \text{ m}^{-1}$	57
Figure V.5 Reactor dimensions for the given catalyst weight and 0.24 sec space velocity	57
Figure V.6 Number of tubes for multiple total reactor diameters	58
Figure V.7 OCM and MDA temperature profile along the catalyst bed for multiple values of U_{overall} ranging from 50 to 15000 $\text{W/m}^2\cdot\text{K}$	59
Figure V.8 Heat transfer resistances across the radius of the reactor	60
Figure V.9 Analysis of multiple parameters on the heat transfer coefficient.....	62
Figure V.10 Schematic diagram of a reactor with homogenously packed catalyst with diluent (a); Two different ways of catalyst profiling (b & c).....	65
Figure V.11 Effect of adding diluents on the temperature profiles of an OCM-MDA reactor with 0% diluents and $U_{\text{overall}} = 400$ and $1000 \text{ W/m}^2\cdot\text{K}$ (left) and 40% diluents with $U_{\text{overall}} = 130, 400$ and $1000 \text{ W/m}^2\cdot\text{K}$ (right)	66
Figure V.12 Catalyst profiling, temperature profiles and reactor performance of the OCM-MDA reactor for 50% gas volume, 0% MDA diluent and OCM 50% homogenous diluent (left), 100 to 0% diluent profiling (middle) and 0 to 100% diluent profiling (right).....	67
Figure V.13 Catalyst profiling, temperature profiles and reactor performance of the OCM-MDA reactor for 50% gas volume, 0% OCM diluent and MDA 40% homogenous diluents (left), 80 to 0% diluent profiling (middle) and 0 to 80% diluent profiling (right)	69
Figure V.14 Comparison of a co- (left) and counter-current (right) reactor temperature and performance profiles	70
Figure V.15 Final results of reactors coupling methodology	73
Figure V.16 Showcase of an autothermal reactor design.....	73
Figure V.17 Coupled reactor temperature profile (left) and performance along the catalyst bed (right)	74

Figure V.18 Showcase of other acceptable autothermal reactor designs	74
Figure VI.1 Graphical results of some kinetic models of OCM	80
Figure VI.2 Graphical result of a kinetic model of OCM	80
Figure VI.3 Graphical results of a kinetic model of OCM.....	80

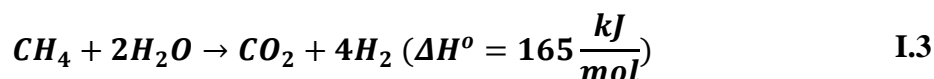
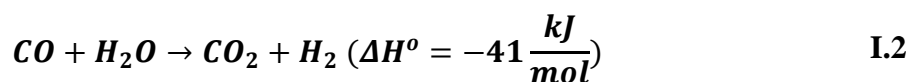
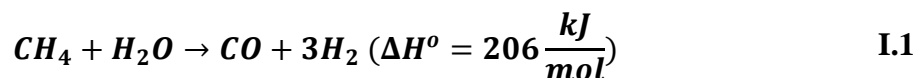
LIST OF TABLES

	Page
Table II.I Literature summary of OCM and MDA kinetic models	24
Table II.II Overview of reported OCM kinetic models in the literature	25
Table II.III Overview of reported MDA kinetic models in the literature.....	26
Table IV.I OCM parametric studies	38
Table IV.II MDA parametric studies	40
Table IV.III Comparison of OCM and MDA parametric studies	41
Table IV.IV Optimization table for one-variable-at-a-time optimization for thermal coupling of OCM-MDA	47
Table IV.V Multiple OCM-MDA thermal coupling case studies.....	49
Table V.I Reactor selection with respect to the heat of reaction.....	51
Table V.II Input variables used for studying the effect of overall heat transfer coefficient	59
Table V.III Input conditions used for calculating heat transfer coefficient from multiple models.....	63
Table V.IV Predicted heat transfer coefficients from multiple correlations from the literature.....	64
Table V.V Input variables used for studying the effect of diluents on the temperature profile.....	66
Table V.VI Input variables for studying the effect of OCM catalyst profiling.....	68
Table V.VII Input variables for studying the effect of MDA catalyst profiling	69
Table V.VIII Input variables for studying the effect of co-current and counter-current reactor designs	70
Table V.IX Base case taken from separate reactors for coupled reactors study	72
Table VI.I Current status and future work for the optimization of reactors.....	77

CHAPTER I
INTRODUCTION

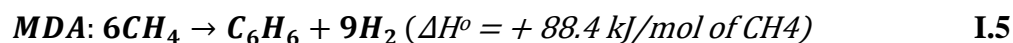
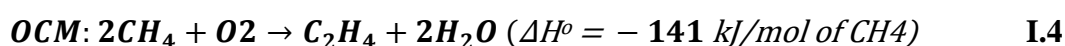
Motivation

Around 50 billion tons of greenhouse gases are emitted throughout the globe, of which 24% account for the industrial carbon emissions. Amongst these emissions, approximately 3 billion tons of carbon dioxide is emitted through the chemical and petrochemical industries [1]. Methane is a major feedstock in many of the chemical and petrochemical industries to produce valuable products as ammonia, methanol, Fischer-Tropsch fuels and olefins. However, all of these processes are considered indirect routes as require making of synthesis gas (CO and H₂) first via methane reforming, followed then by other chemical plants. The reforming reactions are shown below:



In these reactions, around 5.5 kg CO₂/kg H₂ is produced from the reaction stoichiometry. Whereas, in reality, around 9–14 kg CO₂/kg H₂ is generated depending on the energy sources used and efficiency. [2] This industrial carbon emission directly impacts our global climate. The use of direct conversion of methane to valuable products is a promising route to reduce the emissions of CO₂ and simplify the economical and

environmental footprint of the chemical plants. Such direct processes include Oxidative Coupling of Methane (OCM) and Methane DehydroAromatization (MDA). OCM uses oxygen to couple methane into higher hydrocarbons like ethane, ethylene, propane, etc. Whereas, MDA is a process that occurs in absence of oxygen to produce higher hydrocarbons, such as benzene, toluene, naphthalene, etc. The two key reactions for OCM and MDA are shown below:



However, owing to high energy demands and challenges, these processes are not yet able to compete with the existing industrial processes that use indirect conversion processes. OCM requires rigorous heat management since it is highly exothermic. It has low C₂₊ selectivity and methane conversion due to the formation of CO_xs. Whereas, MDA requires high temperature and is an endothermic reaction. In addition, it has fast catalyst deactivation and low methane conversion and yield owing to thermodynamic limitations. [3] Many catalysts for OCM have been tested in the literature that include Li/MgO, La₂O₃/CaO, etc. as shown in fig. I.1 [4]. Whereas, for MDA multiple the mostly used catalysts are Mo/HZSM-5 and Mo/HMCM-22, besides multiple other reported catalysts [5].

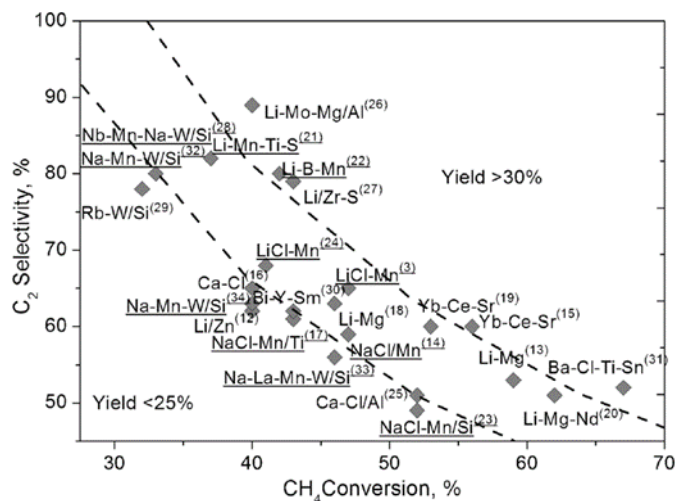


Figure I.1 Multiple OCM catalysts reported in the literature [4]

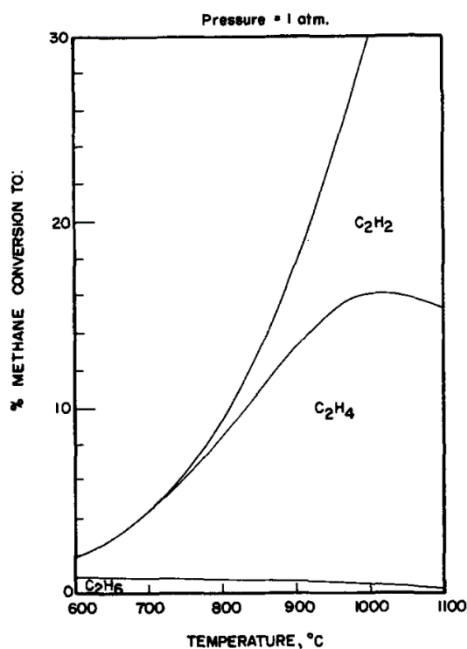


Figure I.2 Methane conversion of OCM at multiple operating temperatures [6]

OCM and MDA, both have similar operating conditions from 650 to 850 °C and 1 atm, as shown in the fig I.2 and fig. I.3. [6], [7].

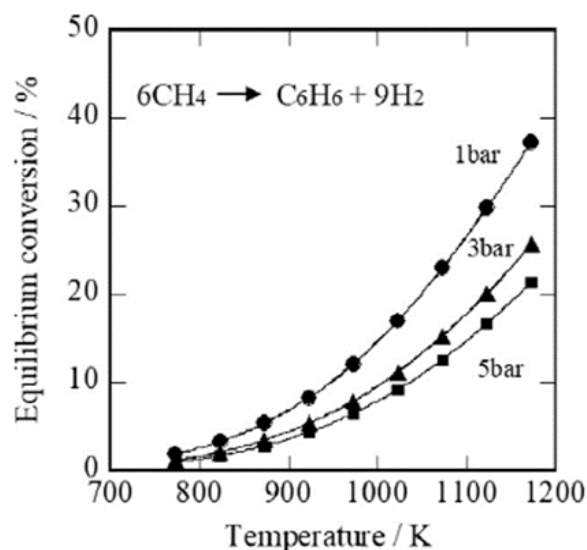


Figure I.3 Equilibrium methane conversion of MDA at multiple operating temperatures [7]

OCM and MDA have their own technical challenges as presented earlier that prevent them from commercialization. In this work we believe that by considering these two processes under one umbrella, one can overcome some of the main technical challenges for both processes. And this is mainly due to three reasons. Firstly, it can help in terms of heat management, as OCM is highly exothermic and requires good temperature control to avoid runaway reaction. Whereas, MDA is a highly endothermic reaction and requires a significant amount of energy to proceed. Thereby, both reactions can form an exothermic-endothermic system, with the possibility to generate an autothermal operation. Secondly, they have similar components and similar operating conditions. This can be beneficial, while being in the same chemical plant, in terms of design and operations. Thereby, reduce overall plant costing. Thirdly and most importantly, both the reactions

are direct conversions, therefore, overall CO₂ emissions per final products could be significantly reduced.

There can be multiple integration options possible between these two reaction routes:

Mass integration option: In this case, both reactions can be carried out in same reactor and the outlet from OCM goes to the MDA catalyst as shown in fig. I.4a.

Process integration option: In this case, integration is done on the reactor inlet and outlet streams while using heat exchanger outside reactor as shown in fig. I.4b.

Reactors heat integration option: In this case, heat is exchanged between the OCM and MDA reactor such that heat requirement of MDA is fulfilled by the heat released by OCM. As shown in the heat integration option, fig. 1.4c, each reaction takes place in separate channel separated by a wall. The heat from OCM drives towards MDA. Both the catalysts and reactions need to be at a similar temperature range. The temperature profiles, that include axial and radial, becomes important in this case.

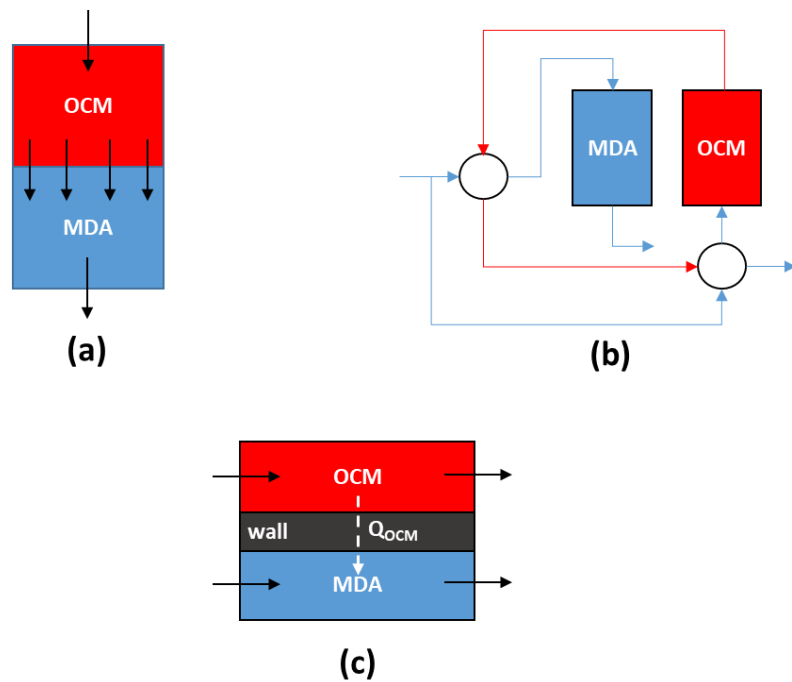


Figure I.4 Multiple integration options for OCM and MDA (a) Mass integration option; (b) Process integration option (c) Reactors' heat integration option

Research objectives

In this research work, thermal coupling of OCM and MDA reactions in the same reactor will be studied. Only integration option 3 will be studied in this work. Mass integration and process integration will be outside the scope of this process. The objectives are defined in terms of research questions that will be explored in this work are as follows:

1. Can both reactions be thermally coupled in a single reactor?
2. What is the operating window and conditions required for the thermal coupling?
3. What are the opportunities and limitations for this concept?
4. Can we develop a methodology to design such a synergetic reactor?

Research plan

To answer these research questions, the target is to achieve a coupled reactor design as shown in fig. 1.4 (c). To achieve such a reactor design, a separate reactor model will be built for each, OCM and MDA fig. 1.4 (b). Each of these separate reactor models require a kinetic model for OCM and MDA fig. 1.4 (a). These kinetic models can be identified through the literature.

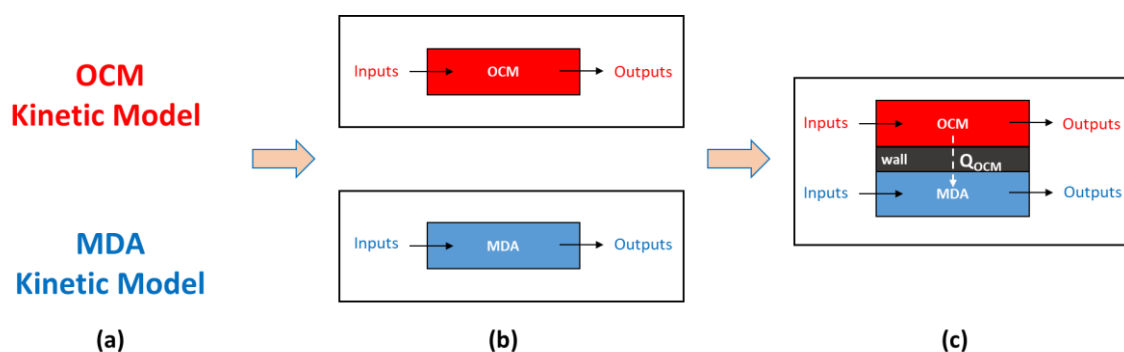


Figure I.5 Kinetic models of OCM and MDA (a); Two separate reactor models for OCM and MDA (b); OCM-MDA coupled reactor design (c)

Thus, the workflow and methodology of this work are structured as shown in fig 1.5.

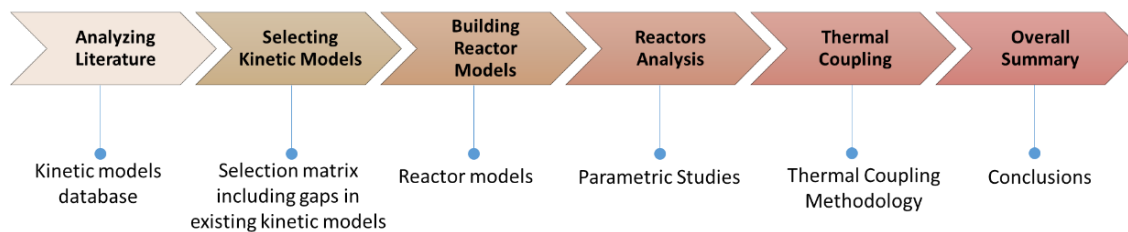


Figure I.6 Research flow chart with deliverables

CHAPTER II

LITERATURE REVIEW

General overview

Thermal coupling in this work will be studied mathematically by establishing two 1-D pseudo homogenous packed bed reactor models – one for OCM and another for MDA. Building these reactor model requires the availability of kinetic models. A literature review was conducted to identify all of the available kinetics models of OCM and MDA reactions. The first reported kinetic models for these reactions was found to date back to the early 1980s. Simple empirical kinetics to very detailed microkinetic models were found for these two reactions. For OCM around 30 kinetic models were identified out of which 17 are empirical models and the rest are microkinetic models. Whereas for MDA, 12 models were collected out of which 7 are empirical models while the rest are microkinetic models. An overview summary of the found OCM and MDA kinetic models is given in the table II.I below:

Table II.I Literature summary of OCM and MDA kinetic models

	OCM	MDA
Date	1988 – 2020	1990 – 2020
Total Kinetic Models	30	12
Empirical Models		
Number of models	17	7
Reactions	2 – 16	1 – 6
Components	2 – 10	3 – 7
Catalysts	Li/MgO, La ₂ O ₃ /MgO, Sn/Li/MgO, La/MgO, CaTiO ₃ , SnBaTiO ₃ , Mn/Na ₂ WO ₄ /SiO ₂ , NaOH/CaO, La ₂ O ₃ /CaO, La/Sr/Co/Fe/O, Sr/La ₂ O ₃ , PbO/ r-alumina	Ru/Mo/HZSM-5, Mo/HZSM-5, MoO ₃ /ZrO ₂ /ZnO ₂ /bentonite
Microkinetic Models		
Number of models	13	5
Reactions	3 – 164	23 – 54
Components	2 – 28	24 – 30
Catalysts	Na/MgO, Li/MgO, La/MgO, TiSi ₂ /MgO, CoSi ₂ /MgO, Na/BaTiO ₃ /MgO, Na/NiTiO ₃ , Li/NiTiO ₃ , Sr/La ₂ O ₃ , Mn/Na ₂ WO ₄ /SiO ₂	Mo/HMCM-22, Mo ₂ C/HZSM-5
Validity Range - Temperature (K)	923 – 1173 A few (773-1273)	873 – 1023 A few (773 – 1073)
Validity Range – Pressure (atm)	0.864 – 4.046 One upto 40.4	0.987 – 1 one has 0.58
Catalyst deactivation	No	Yes
Reactors	Fixed Bed Reactor (FBR) Membrane FBR Fluidized Bed reactor	Fixed Bed Reactor (FBR) Membrane FBR
No. of experiments	10 – 175	10 – 21

OCM kinetic models

Most of the kinetic models reported for OCM are reported in table II.II. The most reported kinetic models are for Li/MgO and Mn/Na₂WO₄/SiO₂. The validity ranges lie mostly in between 750 – 900 °C whereas a few also range from 500 – 1000 °C. In terms of pressure, kinetic models usually refer to atmospheric conditions, however data is also found from 0.85 – 4 atm and extreme pressures like 40 atm as well. Components that have been catered in the empirical kinetic models include, CH₄, O₂, C₂H₆, C₂H₄, C₃H₈, C₃H₆, CO, CO₂, H₂ and H₂O. Multiple reactions have been proposed for each of these models ranging from 2 to 16. Whereas, neither of the models take account of the catalyst deactivation. Most of them have utilized a fixed bed reactor; while some work is also

reported for membrane bed reactors, a few have also utilized fluidized bed reactor for kinetic testing for the model development. Number of experimentations reported for kinetic testing can be seen as low as 10 and as high as 175. A brief overview of these models is shown below:

Table II.II Overview of reported OCM kinetic models in the literature

#	Year	Author	Catalyst	Model
OCM-1	1988	V. T. Amorebieta [8]	7% Li-MgO	Empirical
OCM-2	1988	J. M. Deboy [9]	1 wt% Sr/La ₂ O ₃	Empirical
OCM-3	1989	E. Iwamatsu [10]	15% Na ⁺ -MgO catalyst	Microkinetic
OCM-4	1989	J. A. Roos [11]	2.8 wt.% Li / 8.2 wt.% CO ₂	Microkinetic
OCM-5	1990	E. E. Miro [12]	0.5, 5.4, 7.6, 9.7, 13.8% Li/NiTiO ₃ 1.6, 8.7, 14, 22, 32% Na/NiTiO ₃	Microkinetic
OCM-6	1990	H. Zanthoff [13]	-	Microkinetic
OCM-7	1991	Y. Feng [14]	1% Sr/La ₂ O ₃	Microkinetic
OCM-8	1992	L. Lehmann [15]	11 mol% NaOH/CaO	Empirical
OCM-9	1993	S. C. Reyes [16]	-	Microkinetic
OCM-10	1995	S. Cheng [17]	34 wt% PbO/ r-alumina	Empirical
OCM-11	1995	W. Wang [18]	3 % Li/MgO	Empirical
OCM-12	1996	U. Pannek [19]	La ₂ O ₃ /CaO	Empirical
OCM-13	1996	M. Sohrab [20]	CaTiO ₃	Empirical
OCM-14	1997	Z. Stansch [21]	La ₂ O ₃ (27 at. %)/CaO	Empirical
OCM-15	1998	Yu. I. Pyatnitsky [22]	10% La ₂ O ₃ /MgO	Empirical
OCM-16	1998	M. Traykova [23]	TiSi ₂ (0.53 m ² /g)/MgO CoSi ₂ (2.01 m ² /g)/MgO	Microkinetic
OCM-17	2006	N. S. Matin [24]	Na/BaTiO ₃ /MgO	Microkinetic
OCM-18	2006	J. A. Langille [25]	2 wt% Mn/ 5 wt% Na ₂ WO ₄ /SiO ₂	Empirical
OCM-19	2008	J. Sun [26]	Li/MgO and Sn/Li/MgO	Microkinetic
OCM-20	2008	N. Yaghobi [27]	SnBaTiO ₃	Empirical
OCM-21	2009	M. Daneshpayeh [28]	4 wt.% Mn-5 wt.% Na ₂ WO ₄	Empirical
OCM-22	2009	K.Takanabe [29]	La _{0.6} /Sr _{0.4} /Co _{0.8} /Fe _{0.2} /O _{3-d}	Empirical
OCM-23	2009	Z. Taheri [30]	2wt%Mn and 5wt%Na ₂ WO ₄ /SiO ₂	Microkinetic
OCM-24	2010	N. R. Farooji [31]	SnBaTiO ₃	Empirical
OCM-25	2011	A. Farsi [32]	La(0.6)-Sr(0.4)-Co(0.8)-Fe(0.2)-O(3-δ)	Empirical
OCM-26	2013	V. I. Lomonosova [33]	2 wt% Mn/1.2 wt% Na/2.7 wt% W/SiO ₂	Microkinetic
OCM-27	2013	A. Valadkhani [34]	1% La/MgO (5% Na ₂ WO ₄ , 0.6% Mn) NaWMn/SiO ₂	Microkinetic
OCM-28	2013	J. S. Ahari [35]	Mn/Na ₂ WO ₄ /SiO ₂	Microkinetic
OCM-29	2014	A. Vatani [36]	3.3 wt.% Li/MgO	Empirical
OCM-30	2019	D. Li [37]	-	Microkinetic

MDA kinetic models

Most of the kinetic models reported for MDA are for Mo/HZSM-5 as shown in table II.III. The validity ranges lie mostly in between 600 – 750 °C owing to the increased coking issue that develops at higher temperatures. Whereas a few also range from 500 – 800 °C. In terms of pressure, kinetic models usually refer to atmospheric conditions, however one of the kinetic models have also referred to a lower pressure of 0.58 atm. Components that have been catered in the empirical kinetic models include, CH₄, C₂H₄, C₂H₆, C₆H₆, C₇H₈, C₁₀H₈, H₂ and inert. Multiple reactions have been proposed for each of these models ranging from 1 to 6. While majority of the kinetic models do not involve catalyst deactivation, some of the models also include the phase of deactivation. Most of them have utilized a fixed bed reactor, while some also utilize membrane bed reactors for kinetic testing for the model development. Number of experimental data points reported for kinetic testing can be seen from 10 to 21.

Table II.III Overview of reported MDA kinetic models in the literature

#	Year	Author	Catalyst	Model
MDA-1	1990	A. M. Dean [38]	-	Microkinetic
MDA-2	2001	O. Rival [39]	-	Microkinetic
MDA-3	2001	L. Li [40]	0.5% Ru-3% Mo/HZSM-5	Empirical
MDA-4	2002	L. Li [41]	Mo/HZSM-5	Empirical
MDA-5	2003	M. C. Iliuta [42]	0.5% Ru-3% Mo/HZSM-5	Empirical
MDA-6	2008	B. Yao [43]	modified Mo/HZSM-5	Empirical
MDA-7	2012	K. S. Wong [44]	5.3 wt.%Mo/HMCM-22 with Si/Al ratio of 15.5	Microkinetic
MDA-8	2015	C. Karakaya [45]	Mo ₂ C/HZSM-5	Microkinetic
MDA-9	2016	C. Karakaya [46]	6 wt % Mo/HZSM-5	Microkinetic
MDA-10	2017	N. I. Fayzullaev [47]	(MoO ₃) _x ·(ZrO ₂) _y ·(ZnO ₂) _z /bentonite	Empirical
MDA-11	2018	Y. Zhu [48]	6 wt% Mo/HZSM-5	Empirical
MDA-12	2020	J. Jeong [49]	bulk Mo content of 5.94 wt.%/HZSM-5	Empirical

A matrix for selection of kinetic models to be used in this work

In the start of the work, a few kinetic models for OCM and MDA were selected based on the following criteria:

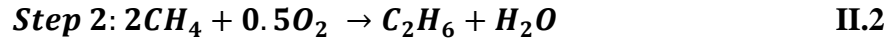
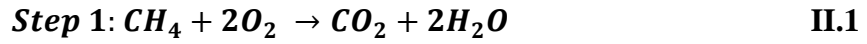
- Availability of kinetic expressions with complete information of the expression and its parameters
- Validity range of the kinetic model for the given compositions, flowrate, temperature, and pressure
- Availability of a correct and usable experimental data for model validation
- Availability of complete definitions of reactor performances and model results, like conversion, selectivity, and yield.

Based on this selection matrix, six out of seventeen empirical models of OCM and four out of seven empirical kinetic models of MDA were tried to reproduce. One model of each reaction was successfully reproduced, 3% Li/MgO for OCM and 6% Mo/HZSM-5 for MDA. These models are used to build the reactor models used to establish the thermal coupling methodology. Full explanation of the used kinetic models is given ahead.

OCM kinetic model

The kinetics of OCM on 3% Li/MgO involves 4 components, CH₄, O₂, C₂H₆ and CO₂. It is a 2-reaction global kinetic model [18]. It describes the differential rate of formation for different components under the range of experimental conditions of 1 atm, 873 – 1023 K, 1000 cm³ (STP)/min with the feed compositions of CH₄: 2.5 – 35% and O₂: 0.12 – 3.2%. The catalyst bulk density is taken as 345 kg/m³. The kinetic model includes ethane formation through oxidative coupling reaction of methane and a complete

oxidation step of methane forming carbon dioxide. This model assumes that all C₂ products as C₂H₆ and all side products being CO_xs as CO₂. However, these assumptions are valid since other products like C₂H₄ and CO were not observed under the given experimental conditions of low residence times, hence were considered secondary reactions and not included in this global kinetic model. The kinetic model considers the following set of stoichiometric equations:



The reaction rates for each step are given below:

$$r_{1, CO_2} = \frac{k_3 p_{O_2}^{1.251}}{4} \left[\left(1 + \frac{8 k_2 \frac{C_P}{C_T} p_{CH_4}}{k_3 p_{O_2}^{1.251}} \right)^{0.5} - 1 \right] + 16 S_0 k_2 \frac{C_P}{C_T} p_{C_2} \left(\frac{\text{mol } CO_2}{\text{cm}^3 \cdot \text{s}} \right) \quad \text{II.3}$$

$$r_{2, C_2H_6} = \frac{k_3 p_{O_2}^{1.251}}{16} \left[\left(1 + \frac{8 k_2 \frac{C_P}{C_T} p_{CH_4}}{k_3 p_{O_2}^{1.251}} \right)^{0.5} - 1 \right]^2 + 8 S_0 k_2 \frac{C_P}{C_T} p_{C_2} \left(\frac{\text{mol } C_2H_6}{\text{cm}^3 \cdot \text{s}} \right) \quad \text{II.4}$$

Where, C_P and C_T are electron-hole concentration and total concentration of all defects in the catalyst respectively and are determined by the partial pressures of reactants and products and S₀ is the fraction of radicals that undergoes deep oxidation reaction, given as:

$$\frac{C_P}{C_T} = \frac{k_1 pO_2^{0.5}}{k_1 pO_2^{0.5} + k_1 k_2 k_4 + k_2 (pCH_4 + 8 S_0 pC_2)} \quad \text{II.5}$$

$$S_0 = 2 \left(1 + 8 Z \frac{k_2 pCH_4^{0.5}}{k_3 pO_2^{1.251}} + 1 \right) \quad \text{II.6}$$

$$Z = \frac{k_1 pO_2^{0.5}}{k_1 pO_2^{0.5} + k_1 k_2 k_4 + k_2 pCH_4} \quad \text{II.7}$$

The kinetic parameters used in this kinetic model were obtained by (Wang and Lin, 1995)[18] by performing linear regression of experimental data (Tung and Lobban, 1992) [50]. The units of activation energy are kcal/mol. The kinetic parameters of this kinetic model are shown below:

$$k_1 = 2.472 * 10^7 \exp\left(-\frac{49.64}{RT}\right) \left(\frac{\text{mol}}{\text{cm}^3 \text{s}}\right) \quad \text{II.8}$$

$$k_2 = 10.10 \exp\left(-\frac{23.15}{RT}\right) \left(\frac{\text{mol}}{\text{cm}^3 \text{s}}\right) \quad \text{II.9}$$

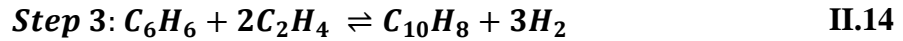
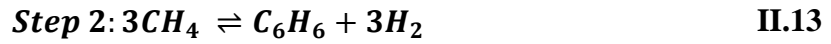
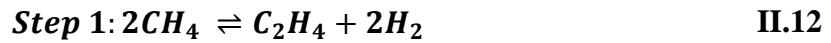
$$k_3 = 1.103 * 10^{-3} \exp\left(-\frac{4.548}{RT}\right) \left(\frac{\text{mol}}{\text{cm}^3 \text{s}}\right) \quad \text{II.10}$$

$$k_4 = 2.093 * 10^{-4} \exp\left(\frac{27.94}{RT}\right) \left(\frac{\text{mol}}{\text{cm}^3 \text{s}}\right) \quad \text{II.11}$$

MDA kinetic model

The kinetics of MDA on 6% Mo/HZSM-5 involves 5 components, CH₄, C₂H₄, C₆H₆, C₁₀H₈ and H₂. It is a 3-reaction global kinetic model [48]. It describes the differential

rate of formation for different components under the range of experimental conditions of 1 atm, 948 – 1023 K, WHSV of 750 – 3000 ml/g.h with the feed composition of 95% CH₄ balanced with the He as inert. The catalyst density is taken as 510 kg/m³. The kinetic model includes formation of major products, olefins as ethylene and, aromatics as benzene and naphthalene, through non-oxidative coupling reaction of methane. However, this model does not include deactivation of catalyst and other reaction products. The kinetic model considers the following set of stoichiometric equations:



The reaction rates for each step are given below:

$$r_{1,\text{C}_2\text{H}_4} = k_{f1} p\text{CH}_4 (1 - \eta_1) \left(\text{mol} \frac{\text{C}_2\text{H}_4}{\text{g}_{\text{cat}} \text{h}} \right) \quad \text{II.15}$$

$$r_{2,\text{C}_6\text{H}_6} = k_{f2} p\text{C}_2\text{H}_4 (1 - \eta_2) \left(\text{mol} \frac{\text{C}_2\text{H}_6}{\text{g}_{\text{cat}} \text{h}} \right) \quad \text{II.16}$$

$$r_{3,\text{C}_{10}\text{H}_8} = k_{f3} p\text{C}_2\text{H}_4 p\text{C}_6\text{H}_6 (1 - \eta_3) \left(\text{mol} \frac{\text{C}_{10}\text{H}_8}{\text{g}_{\text{cat}} \text{h}} \right) \quad \text{II.17}$$

Where, η_i is the approach to equilibrium. It indicates if the direction of the reaction rate: Forward reaction rate when $\eta_i < 1$ and backward reaction rate when $\eta_i > 1$. It is defined by:

$$\eta_1 = \frac{pC_2H_4 pH_2^2}{K_{p1} pCH_4^2} \quad \text{II.18}$$

$$\eta_2 = \frac{pC_6H_6 pH_2^3}{K_{p2} pC_2H_4^3} \quad \text{II.19}$$

$$\eta_3 = \frac{pC_{10}H_8 pH_2^3}{K_{p3} pC_6H_6 pC_2H_4^2} \quad \text{II.20}$$

Kinetic models validation

The kinetic models for OCM and MDA were reproduced and validated using the kinetic models' papers. OCM kinetic model was validated with the experimental data [18] and the simulation results reported elsewhere [51]. A good fit was obtained and can be seen in the figures III.1 and III.2:

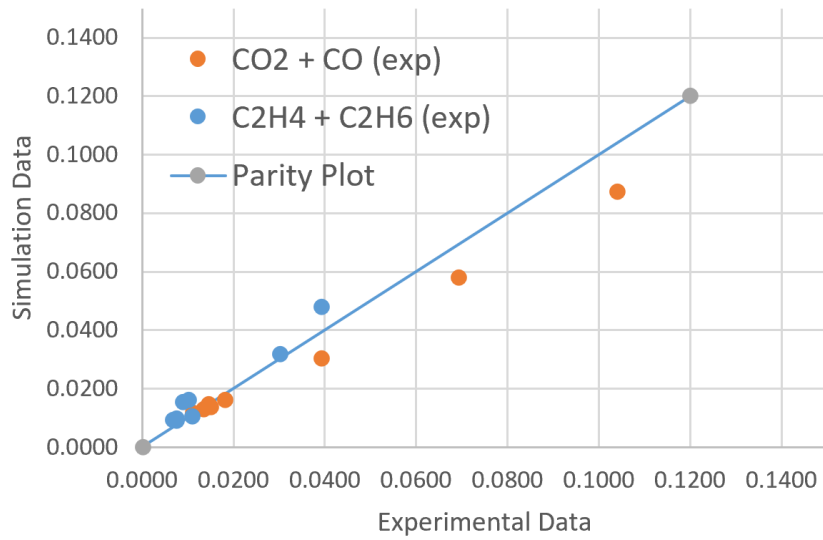


Figure II.1 (Wang, 1995) Experimental data vs Our simulation

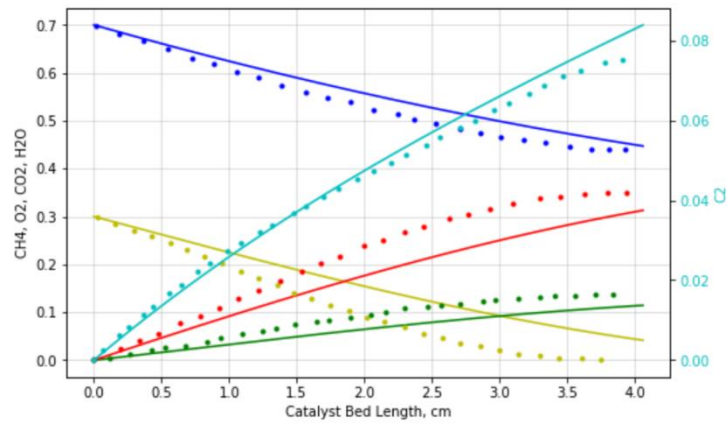


Figure II.2 (Kao, 1997) Simulation (.) vs Our simulation (—)

Similarly, the MDA kinetic model was validated by comparing with the simulation results of Zhu [48] and Microkinetic Model by Karakaya [46]. A good fit was obtained and can be seen in the figures III.3 and III.4:

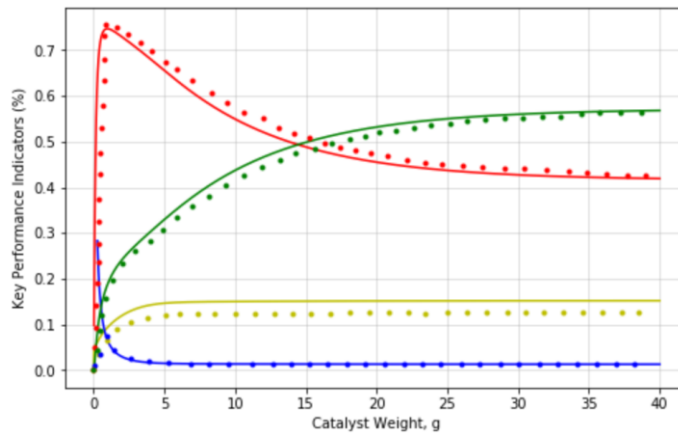


Figure II.3 (Zhu, 2018) Simulation vs Our simulation

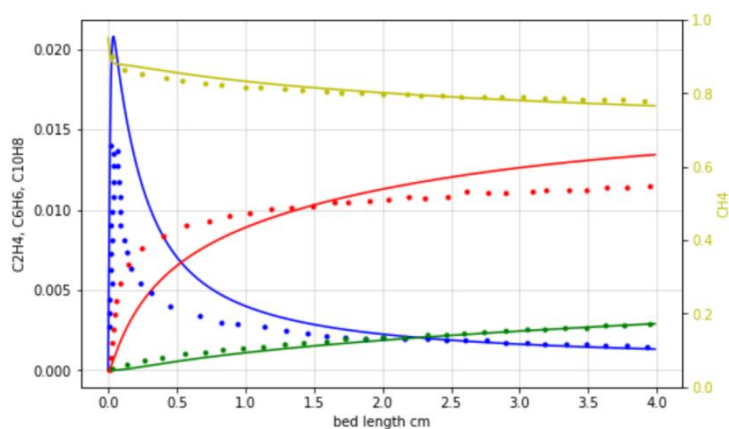


Figure II.4 (Karakaya, 2016) Microkinetic model vs Our simulation

A good comparison of our simulation versus the Microkinetic model showed that this global kinetic model was able to capture the trends as depicted by the Microkinetic model. Further, to see how our model results compares to another model, this kinetic model was compared to the kinetic model of Iliuta [42]. The same catalyst, 6% Mo/HZSM-5, was used by Iliuta with simulation conditions of 700 °C, 101 kPa, 0.225 cm³/s and feed composition as 79% CH₄ and 21% inert. The catalyst weight was compared by our simulation to reach a target conversion of 11%. Our simulation predicted 1 g of 6% Mo/HZSM-5 catalyst versus their result as 3 g. Hence, based on the ability to capture the trend of a microkinetic model and showing a good order of magnitude estimate, this kinetic model was selected for establishing the methodology of thermal coupling.

CHAPTER III

MATHEMATICAL MODELING OF SEPARATE 1-D PSEUDO HOMOGENOUS IDEAL PACKED BED REACTOR MODELS

Schematic diagram of a thermally coupled OCM-MDA reactor, and how the reactor model was developed is shown in Figure III.1.

The following assumptions were used to build the reactor models.

1. The system is in steady state condition
2. The system is isothermal and isobaric
3. Physical properties of the catalyst are fixed
4. No heat and mass transfer limitations
5. No effect of axial dispersion

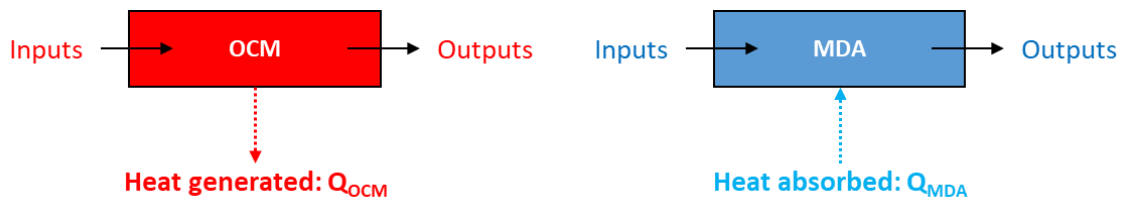


Figure III.1 Schematic diagram of separate OCM reactor (left) and MDA reactor (right)

Reactor design equations

Based on the reactor model assumptions and employing law of conservation of mass and energy, the following balances can be modeled:

Mole Balance:

$$\frac{dF_i}{dW} = r_{i,net} \quad \text{III.1}$$

Energy balance:

$$Q_{g,n} = \sum^n (\Delta H_{j,i} * r_{j,i}) \quad \text{III.2}$$

$$\Delta H_{j,i} = \Delta H_{j,i}^o + \Delta C_{P,j,i}(T_n - T_R) \quad \text{III.3}$$

$$\Delta H_{j,i}^o = \sum H_{f,i}^P - \sum H_{f,i}^R \quad \text{III.4}$$

$$\Delta C_{P,j,i} = \sum \left(\frac{\theta_i}{\theta_a} C_{P,i} \right)^P - \sum \left(\frac{\theta_i}{\theta_a} C_{P,i} \right)^R \quad \text{III.5}$$

The amount of heat generated or absorbed by the reactions is calculated by equation III.5.

Numerical solution

In this study, the mathematical model consists of a set of algebraic and ordinary differential equations, solved using Python environment. The ODEs were solved using ODEINT function which basically uses the Livermore Solver for Ordinary Differential Equations. The thermodynamic data was retrieved using Thermochem Package which is a Python Thermodynamic Library. This library was interlinked within the Python code such that it retrieves data and properties at any given point of operating condition. The model flowchart is shown below:

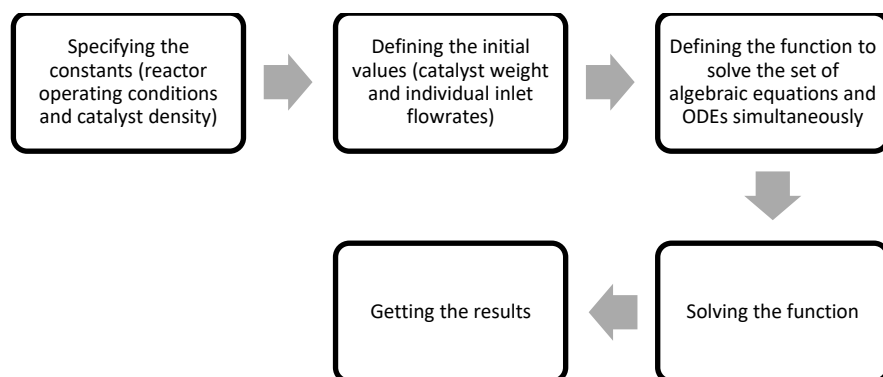


Figure III.2 Model flow chart for obtaining the numerical solution

Reactions' parameter calculation

The conversion, selectivity and yield of the components used in this research work are defined as:

$$\text{Conversion \% (i)} = \frac{F_{i,in} - F_{i,out}}{F_{i,in}} * 100 \quad \text{III.6}$$

i: CH₄, O₂

$$\text{Selectivity \% (i)} = iC * \frac{F_{i,out}}{F_{i,in} - F_{i,out}} \quad \text{III.7}$$

iC: number of Carbons in the component j

i: C₂H₄, C₂H₆, C₆H₆, C₁₀H₈

$$\text{Yield (i)\%} = \text{Selectivity (i)} * \text{Conversion (CH}_4) * 100 \quad \text{III.8}$$

CHAPTER IV

THERMAL COUPLING OF SEPARATE OCM AND MDA REACTORS

Now that the separate reactor models of OCM and MDA are established, this section presents a parametric study on each reactor separately. This is required to understand how each reactor parameter affect the reaction performance and its heating requirements so that both reactions can be coupled in a single reactor.

Parametric studies of OCM

Table IV.1 shows the parametric study result for OCM case. A reference base was first defined at an input feed flowrate of 10,000 std. m³/h basing on a medium scale industrial plant. The temperature and pressure, 700 °C and 1 atm, is chosen conservatively at the lower side, such that changes could be studied by increasing such conditions and comparing them to this base case. The feed composition of methane and inerts are taken to have a feed ratio of methane-to-oxygen to 3. The catalyst weight was varied to obtain a C₂ yield of around 20%, and methane and oxygen conversion of 33% and 94%, and a C₂ selectivity of around 60%. The heat duty was then recorded as approximately 9.5 MW for such given conditions.

Table IV.I OCM parametric studies

Cases	Operating Conditions				Feed Composition			Reactor Performance				Heat, Cat. Wt.		Summary
	F	T	P	GHSV	Y _{CH4}	Y _{CH4/O2}	Y _{Inert}	Y _{C2}	X _{CH4}	X _{O2}	S _{C2}	Q	m _{cat}	
	Std m ³ /h	°C	atm	h ⁻¹	%	-	%	%	%	%	%	MW	tons	
Base Case	10,000	700	1	6,900	61.7	3	17.8	19.6	32.8	94.3	59.8	9.52	0.5	
↑GHSV: 2X Flow	↑20,000	700	1	13,800	61.7	3	17.8	↓11.4	↓20.0	↓60.3	↓57.1	↑12.54	0.5	↑Flow ↑Heat ↓RPs
↑GHSV: ½ Cat. Wt.	10,000	700	1	13,800	61.7	3	17.8	↓11.4	↓20.0	↓60.3	↓57.1	↓6.26	↓0.25	↓Catalyst ↓Heat ↓RPs
↑Pressure: 5X	10,000	700	↑5	6,900	61.7	3	17.8	↓16.3	↓30.8	↑99.99	↓52.8	↑10.1	0.5	↑Pressure ↑Heat ↑X _{O2} ↓Wt.
↑Temperature: +100	10,000	↑800	1	6,900	61.7	3	17.8	↑33.8	↑46.1	↑99.99	↑73.2	↑9.95	0.5	↑Temp. ↑Heat ↑RPs ↓Wt.
↑Inerts: 2.3X	10,000	700	1	6,900	45	3	↑40	↑20.9	↑34.1	↑94.9	↑61.3	↓7.1	0.5	↑Inerts ↓Heat ↑RPs
↓Inerts: 1.8X	10,000	700	1	6,900	67.5	3	↓10	↓19.2	↓32.5	↓93.96	↓59.1	↑10.4	0.5	↓Inerts ↑Heat ↓RPs
↑CH ₄ /O ₂ Ratio: 1.7X	10,000	700	1	6,900	68.48	↑5	17.8	↓18.4	↓26.0	↑99.5	↑70.6	↓6.61	0.5	↑Ratio ↓Heat ↑X _{O2} ↑S _{C2}
↓CH ₄ /O ₂ Ratio: 2X	10,000	700	1	6,900	49.3	↓1.5	17.8	↓16.3	↑39.9	↓77.2	↓40.7	↑13.1	0.5	↓Ratio ↑Heat ↑X _{CH4}

Effect of gas hourly space velocity

Gas Hourly Space Velocity (GHSV) can be increased by either increasing the feed flowrate or by decreasing the catalyst weight. Both of such ways are studied to see the difference in the effects. By increasing the feed flowrate to double, all the reactor performances were severely decreased whereas, heat duty showed an increase. On the other hand, by decreasing the catalyst weight to half, all the reactor performances remained the same as were by increasing the flow rate to the same GHSV, however the heat duty showed a significant decrease. Such a difference in the effects of both ways can be explained by the increase in concentrations of the reactants caused due to the increase in feed flowrate, whereby on the other case, the reactants concentration remains the same by decreasing the catalyst weight, thereby decreasing the overall reactor performance. Therefore, as the effect of both the ways is different, hence, while the GHSV can be increased, the heat duty can be adjusted either increased or decreased as needed.

Effect of pressure and temperature

By increasing the pressure five times, all the reactor performances, except the oxygen conversion, showed a significant decrease in their values. The reactor heat duty also decreased but was not so significantly. Another impact of increasing pressure was that an excess amount of catalyst could be saved, that is, required catalyst weight was decreased to 0.182 tons for the complete conversion of oxygen. However, the reactor was run completely till 0.5 tons of catalyst to maintain studying the effect of only one parameter at a time. But since one of the reactants was consumed, hence no further change in the reactor performance or the heat duty was observed after 0.182 tons.

Increasing the temperature by a 100 °C, showed an opposite impact compared to the pressure, in terms of the reactor performances. All the reactor performances showed a significant increase along with the heat duty. In terms of the catalyst weight, it showed a similar trend of having an excess catalyst weight and a complete oxygen conversion was achieved at 0.185 weight of the catalyst.

Effect of feed composition

Increasing the amounts of inerts, while fixing the methane-to-oxygen feed ratio at 3, shows a slight increase in the reactor performances, but decreases the heat duty with a huge impact. And an opposite behavior is observed when the inerts are decreased.

On the other hand, when the methane-to-oxygen feed ratio is varied while fixing the amount of inerts in the feed, an increase in the ratio depicts an increase in the selectivity of C₂, whereas a decrease in the ratio depicts an increase in the conversion of methane. Hence, to achieve the same amount of yield, the ratio can either be increased or decreased,

while being able to achieve either a higher C2 selectivity with lower methane conversion, or lower C2 selectivity with a higher methane conversion.

Parametric studies of MDA

Similar to the parametric study of OCM, an MDA study was conducted as shown in Table IV.3. The MDA reference base case for MDA was chosen similar to that of OCM to allow for comparison later on. The temperature and pressure were chosen as 700 C and 1 atm, since these conditions are generally reported in the literature. The feed composition was chosen as 95% methane to be able to also study the effect of inerts. Further, the catalyst weight was varied to achieve around 8% of methane conversion. The heat duty obtained was around 1 MW.

Table IV.II MDA parametric studies

Cases	Operating Conditions				Feed Composition		Reactor Performance			Heat, Cat. Wt.		Summary
	F	T	P	GHSV	Y _{CH4}	Y _{inert}	Y _{C6}	X _{CH4}	S _{C6}	Q	m _{Cat}	
	Std m ³ /h	°C	atm	h ⁻¹	%	%	%	%	%	MW	tons	
Base Case	10,000	700	1	832	95	5	0.98	8.2	12.0	0.92	6.13	
↑GHSV: 2X Flow	↑20,000	700	1	1,664	95	5	↓0.6	↓6.4	↓8.8	↑1.45	6.13	↑Flow ↑Heat ↓RPs
↑GHSV: ½ Cat. Wt.	10,000	700	1	1,664	95	5	↓0.6	↓6.4	↓8.8	↓0.72	↓3.07	↓Catalyst ↓Heat ↓RPs
↑Pressure: 5X	10,000	700	↑5	832	95	5	↑2.0	↓6.7	↑30.2	↓0.75	6.13	↑Pressure ↓Heat ↓X _{CH4}
↑Temperature: +100	10,000	↑800	1	832	95	5	↑3.0	↑19.9	↑15.1	↑2.2	6.13	↑Temp. ↑Heat ↑RPs
↑Inerts: 10X	10,000	700	1	832	50	↑50	↓0.9	10.3	8.6	↓0.61	6.13	↑Inerts ↓Heat ↑X _{CH4}
↓Inerts: 5X	10,000	700	1	832	99	↓1	1.0	↓8.1	↑12.2	↑0.94	6.13	↓Inerts ↑Heat ↑S _{C6} ↑Y _{C6}

Effect of gas hourly space velocity

As done for OCM, the effect of GHSV was studied. First, by increasing feed flowrate to double. All the reactor performances decreased, whereas the heat duty was

increased significantly. However, by decreasing the catalyst weight to half, the reactor performances stayed the same, however, the heat duty was decreased significantly.

Effect of pressure and temperature

By increasing the pressure to five times, all the reactor performances show a significant increase, whereas, the methane conversion decreased. The heat duty decreased in this case. On the other hand, by increasing the temperature by 100 C, all the reactor performances showed a significant increase, however selectivity slightly increased.

Effect of feed composition

Increasing the inerts in the feed, slightly increases the methane conversion, however, it decreases the C6 selectivity and the heat duty. Decreasing the inerts slightly increases the selectivity but decreases the conversion. Hence, methane conversion and C6 selectivity can be adjusted by varying the inerts while maintaining the C6 yield.

Comparison of OCM and MDA studies

After individually studying the processes separately, both processes are compared with respect to their reactor performances and heat duties.

Table IV.III Comparison of OCM and MDA parametric studies

		Cases	OCM	MDA
Operating Conditions	Inlet Temperature C		700 – 800	700 – 800
	Inlet Pressure (atm)		1 – 5	1 – 5
	Flow Rate (Std m3/h)		10,000 – 20,000	10,000 – 20,000
	GHSV (h-1)		6,900 – 13,800	831.97 – 1663.95
Feed Composition	Feed CH4 Mole Fraction (%)		45 – 68.48	50 – 99
	Feed CH4/O2 Ratio		1.5 – 5	-
	Feed Inert Mole Fraction (%)		10 – 40	5 – 50
Reactor Performance	C2/C6 Yield (%)		11.4 – 33.8	0.6 – 3.0
	CH4 Conversion (%)		20.0 – 46.1	6.4 – 19.9
	O2 Conversion (%)		60.3 – 99.99	-
	C2/C6 Selectivity (%)		40.7 – 73.2	8.6 – 30.2
Heat & Cat. Wt.	Heat Requirement (MW)		6.26 – 13.10	0.72 – 2.2
	Catalyst Weight (tons)		0.25 – 0.5	3.07 – 6.13

The parametric study from MDA and OCM were compared against each other as shown in Table IV.III. Apart from the effect of pressure, the rest of the effects for both the reactions are similar. The effect of GHSV, temperature and feed composition showed the same trend for reactor performances and heat duties. For the studied conditions, MDA has lower CH₄ conversion compared to OCM, and it requires 5 to 12 times more catalysts than OCM.

Based on the parametric studies and the comparison, the following can be concluded based on the priority of their impact on the reactor heat duty:

1. Adjusting the flow rate and amount of catalyst simultaneously adjusts heat duty significantly while keeping the reactor performance fixed
2. Adjusting the amount of inerts influences the heat significantly, but also has some impact on the reactor performance
3. Adjusting composition greatly influences heat and reactor performance
4. Adjusting temperature and pressure has a significant impact on performance but lower impact on heat duty

Reactors coupling using Neural Network diagram

Several combinations can be carried out to thermally couple OCM with the MDA reactors resulting in many design options which is very difficult to execute in a trial-and-error manner. Therefore, there is a need for a structured methodology to help navigating between the too many options to identify the most optimal design options for thermal coupling. The concept of Artificial Neural Network (ANN) diagram[52] as shown in fig. IV.1 correlates several inputs and output variables in a very structured way. Thereby, also

provides information flow and results. The input layer takes in information from the user and forwards it to the hidden layers. The hidden layers then compute and processes each variable according to the weight assigned and transfers the information to the output layer. The output layer takes the outputs from the ANN and gives it to the user.

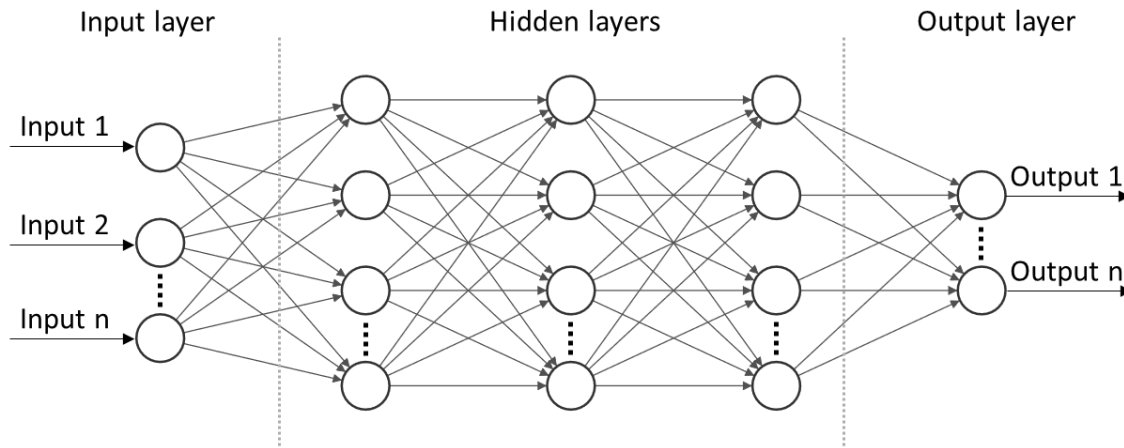


Figure IV.1 Concept of Artificial Neural Network diagram with 'n' multiple inputs and outputs

Inspiration from the analogy of ANN was taken to help establishing a methodology for carrying out the optimization studies toward thermal coupling of OCM and MDA reactors together as shown in fig. IV.2. A physical reactor model is used in this work to link all the input and output variables together. The middle section is used to show the optimized value for the input parameters. These inputs include process operating conditions and design variables like catalyst weight. It also includes the constraints that these input variables can be varied for the required optimization. Initial values along with the optimization priorities are forwarded to the physical reactor model, which is the reactor optimizer. The output layer contains all the reactor outlet parameters such as conversion,

yield and selectivity and heat duties. It shows three columns, the initial values which show the result output from the input initial values; The target column which is used to insert reactor design target parameters; and finally, the optimized column, which shows the final values after full optimization.

Input Layer					OCM-MDA Reactor			Output Layer				
Opt. Priority	Name	Units	Initial Value	Constraints	Optimizer	Optimized Value	Reactor Model	Name	Units	Initial Value	Opt. Value	Target
1	Inlet Temperature	C	800	800		800		C ₂ Yield	%	33.8	33.8	
2	Inlet Pressure	atm	1	1		1		CH ₄ Conv.	%	46.1	46.1	
3	Feed flow rate	Stdm ³ /h	10,000	10,000	Optimizer	10,000	OCM	O ₂ Conv.	%	99.99	99.99	
4	Catalyst weight	tons	0.185	0.185		0.185		Space time	sec	0.24	0.24	
5	Feed composition (Inerts)	%	61.7	61.7		61.7		Heat duty	MW	9.95	9.95	
6	Feed ratio	-	3	3		3		Heat duty	MW	1.15	9.95	Q _{OCM}
7	Inlet Temperature	C	750	T _{OCM}		800		C ₂ Yield	%	1.1	0.95	
8	Inlet Pressure	atm	1	P _{OCM}		1		CH ₄ Conv.	%	10.3	12.3	>10
9	Feed flow rate	Stdm ³ /h	10,000	-	Optimizer	72,320	MDA	Space time	sec	0.98	0.98	
10	Catalyst weight	tons	3	1 - 10		10		Cat. Ratio MDA/OCM	-	16.2	54.1	
11	Feed composition (Inerts)	%	5	< 20		5						

Figure IV.2 Reactors coupling methodology following similar analogy as ANN

A case study using thermal coupling methodology for separate OCM and MDA reactors

This section explains how the design methodology for thermal coupling of OCM and MDA separate reactors work. The methodology is based on manual optimization for now by changing one-variable-at-a-time which will be explained later. A case study is used to explain how this methodology works.

Defining the case study

The feed flowrate of OCM and MDA was taken as the standard of medium-sized plant of 10,000 std.m³/h. The pressure was taken as atmospheric pressure since most of the literature reports this condition. The inerts were maintained on the lower side for higher productivity, hence, less than 20% was chosen for OCM and 5% for MDA. The initial

operating temperatures were chosen between 700 to 800 °C, since this is a common operating window between both the processes. The chosen temperature for OCM was based on at least 30% C₂ yield. The catalyst weight was varied till complete oxygen conversion for OCM and at least 10% CH₄ conversion for MDA. And, based on these inputs, the initial heat duty was calculated for each of the reactors.

Solving the case study using the coupling methodology

The given targets for this case study can be defined as:

- Similar Heat Duty ($Q_{MDA} = Q_{OCM}$)
- Similar Operating Conditions ($T, P_{OCM} = T, P_{MDA}$)
- Low feed inerts
- C₂ Yield for OCM $\geq 30\%$
- CH₄ Conversion for MDA $\geq 10\%$

After the initial values and design targets are defined, the reactor coupling ANN, fig. IV.3 can be partially filled.

There are two reactor models (OCM and MDA) that can be used to do the optimization. Changing both simultaneously can be very complex and it is difficult to execute. Thus, it is better to select one of the reactor models for doing the optimization work while the second reactor is kept fixed as a target.

Selecting the target and the optimizer case

There are two options to select from. Option one is by considering the MDA reactor as target, while OCM can be used as an optimizer. Or option two OCM is a target reactor, while MDA reactor as the optimizer. For the second option to be feasible, the

heat duty of the MDA reactor needs to be lowered from 9.95 MW to 1.15 MW while keeping the C₂ yield greater than 30% and the temperature needs to be lowered from 800 °C to 750 °C. However, lowering the temperature lowers the yield from 30%. In order to lower the heat duty, inerts need to be increased, however, there is a constraint that inerts should remain on the low side, which means they cannot be increased further than 20%. Therefore, this option is not feasible.

The first option is more feasible to select. The heat duty of the OCM reactor needs to be increased from 1.15 MW to 9.95 MW, while keeping the CH₄ conversion greater than 10% and the temperature needs to be increased from 750 °C to 800 °C. The temperature can be increased to 800 °C, which will also assist in increasing the heat duty and further enhance the methane conversion. Another way is to increase the flowrate and to increase the catalyst weight. All these actions shall assist in achieving the targets. Therefore, this option is feasible and can be proceeded further. The above decision was based on the parametric study analysis section carried out which shows that this is an essential step to be carried out.

Manual single-variable-at-a-time optimization

Where multiple-variables-at-a-time optimization can be used in this methodology, currently this research work follows one-variable-at-a-time optimization. Hence, an optimization priority needs to be taken account of since some parameters are hard variables need to be adjusted earlier than later. Amongst these, first, the single-value constraints are first achieved. After which, priority is given to range-constraints. In the given case study, Temperature and Pressure are the single-value constraints and need be

achieved first. However, it can be noticed that only temperature is an input that needs to be changed, and the pressure is already the same as required. Therefore, we prioritize Temperature to be changed first and then proceed for the other parameters that have range-constraints.

For this, we prioritize the parameters that have a higher impact on required performance, such as in this case, the next priority can be given to the catalyst weight and after which are the inerts. If the target is achieved within the optimization of catalyst weight in the given range, the optimizer stops, or else it continues further to the next parameter in line for optimization, which is the catalyst weight.

Thus, this optimization priority shall allow to be in a closer range to the target and constraint by setting the parameters with higher priorities, and the parameters with lower priorities that have lower impact and thus can fine tune the values at later stage. All these were based on the guidelines established in the parametric study.

Once the optimization priority is defined, the optimizer can be run manually. A result of the optimization steps is shown in Table IV.IV. The representation of the results is shown in fig. IV.3:

Table IV.IV Optimization table for one-variable-at-a-time optimization for thermal

Case Description	Operating Conditions				Feed Composition			Reactor Performance				Heat & Cat. Wt.		
	F	T	P	GHSV	Y_{CH_4}	Y_{CH_4/O_2}	Y_{inert}	Y_{C_2/C_6}	X_{CH_4}	X_{O_2}	S_{C_2/C_6}	Q	m_{Cat}	Cat R MDA/OCM
	Stdm ³ /h	°C	atm	h ⁻¹	%	-	%	%	%	%	%	MW	tons	-
OCM (Ref. Case)	10,000	800	1	14,919	61.7	3	17.8	33.8	46.1	99.99	73.2	9.95	0.185	-
MDA (Ref. Case)	10,000	750	1	1,700	95	-	5	1.1	10.3	-	10.3	1.15	3	16.2
MDA (↑F)	72,320	750	1	12,294	95	-	5	0.10	6.4	-	1.5	5.47	3	16.2
MDA (↑T)	72,320	800	1	12,294	95	-	5	0.19	9.6	-	2.0	8.05	3	16.2
MDA (↑Wt.)	72,320	800	1	3,688	95	-	5	0.95	12.3	-	7.6	9.95	10	54.1
MDA (Opt. Case)	72,320	800	1	3,688	95	-	5	0.95	12.3	-	7.6	9.95	10	54.1

Input Layer					OCM-MDA Reactor			Output Layer				
Opt. Priority	Name	Units	Initial Value	Constraints	Optimizer	Optimized Value	Reactor Model	Name	Units	Initial Value	Opt. Value	Target
1	Inlet Temperature	C	800	800		800		C ₂ Yield	%	33.8	33.8	
2	Inlet Pressure	atm	1	1		1		CH ₄ Conv.	%	46.1	46.1	
3	Feed flow rate	Std ³ /h	10,000	10,000	Optimizer	10,000	OCM	O ₂ Conv.	%	99.99	99.99	
4	Catalyst weight	tons	0.185	0.185		0.185		Space time	sec	0.24	0.24	
5	Feed composition (Inerts)	%	61.7	61.7		61.7		Heat duty	MW	9.95	9.95	
6	Feed ratio	-	3	3		3		Heat duty	MW	1.15	9.95	9.95
7	Inlet Temperature	C	750	800		800		C ₆ Yield	%	1.1	0.95	
8	Inlet Pressure	atm	1	1		1		CH ₄ Conv.	%	10.3	12.3	>10
9	Feed flow rate	Std ³ /h	10,000	-	Optimizer	72,320	MDA	Space time	sec	0.98	0.98	
10	Catalyst weight	tons	3	1-10		10		Cat. Ratio MDA/OCM	-	16.2	54.1	
11	Feed composition (Inerts)	%	5	<20		5						

Figure IV.3 Final results of reactors coupling methodology for the given case study

Using of the methodology for other case studies

More of such cases can be developed based on the same methodology. Fig. Table IV.V shows two more cases which were developed for different target temperatures at 750 °C and 850 °C:

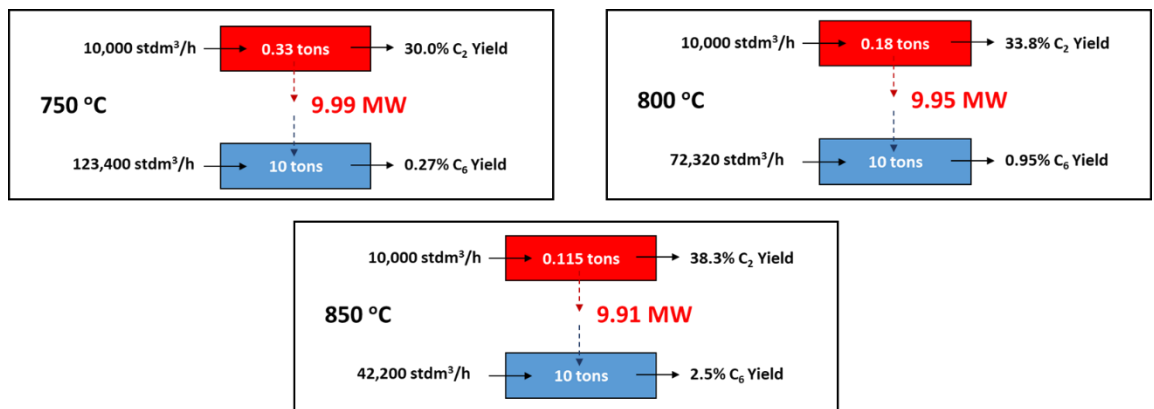


Figure IV.4 Multiple thermally coupled case studies for 700, 800 and 850 °C optimized using the proposed methodology

Table IV.V Multiple OCM-MDA thermal coupling case studies

Case study no.	Cases	Operating Conditions				Feed Composition			Reactor Performance				Heat & Cat. Wt.		
		F	T	P	GHSV	Y _{CH₄}	Y _{CH₄/O₂}	Y _{inert}	Y _{C₂/C₆}	X _{CH₄}	X _{O₂}	S _{C₂/C₆}	Q	m _{Cat}	Cat R
		Stdm ³ /h	°C	atm	h ⁻¹	%	-	%	%	%	%	%	MW	tons	MDA/OCM
1	OCM (Ref. Case)	10,000	800	1	14,919	61.7	3	17.8	33.8	46.1	99.99	73.2	9.95	0.18	54.1
	MDA (Opt. Case)	72,320	800	1	3,688	95	-	5	0.95	12.3	-	7.6	9.95	10	-
2	OCM (Ref. Case)	10,000	750	1	10,455	61.7	3	17.8	30.0	41.7	99.99	68.6	9.99	0.33	30.3
	MDA (Opt. Case)	123,400	750	1	6,923	95	-	5	0.27	10.1	-	3.8	9.99	10	-
3	OCM (Ref. Case)	10,000	850	1	30,000	61.7	3	17.8	38.3	50.2	99.99	76.3	9.91	0.115	86.9
	MDA (Opt. Case)	42,200	850	1	1,085	95	-	5	2.5	21.2	-	11.7	9.91	10	-

It can be observed that all cases can be thermally coupled at different temperatures, 750, 800 and 850 °C. In all the cases, OCM was kept as a reference case, whereas MDA was optimizer. While optimizing MDA, catalyst weight was kept constant at 10 tons and the feed flowrate was changed. As the coupling temperature is increased, the reactor performances increased. The required flowrate for MDA, and thus, the GHSV of MDA is significantly decreased. Whereas the GHSV of OCM significantly rises owing to the lower catalyst weight requirements for achieving the same reactor performances. Finally, it can be noted that the catalyst ratio increases as the coupling temperature is raised, whereby the heat duties are decreased. Such comments can be a guiding path towards the coupled reactors.

CHAPTER V

THERMAL COUPLING OF COUPLED OCM AND MDA REACTORS

So far both OCM and MDA reactor were not coupled, and each reactor was run separately, and metrics were compared. To design a thermally coupled reactor, the OCM reaction needs to be conducted in one compartment of the reactor, while the MDA in the other compartment with a dividing wall in between them, as shown in fig. V.I. The heat is transferred from the OCM compartment to that of the MDA. Through this, it is aimed to run an auto-thermal operation without any additional heating supply or removal. In such a coupled reactor design, the temperature profile cannot be isothermal. Thus, to make this case more realistic, axial temperature profile is being accounted and reactor channel sizing is based on an acceptable pressure drop. This section will explain how a thermally coupled reactor of OCM and MDA can be designed.

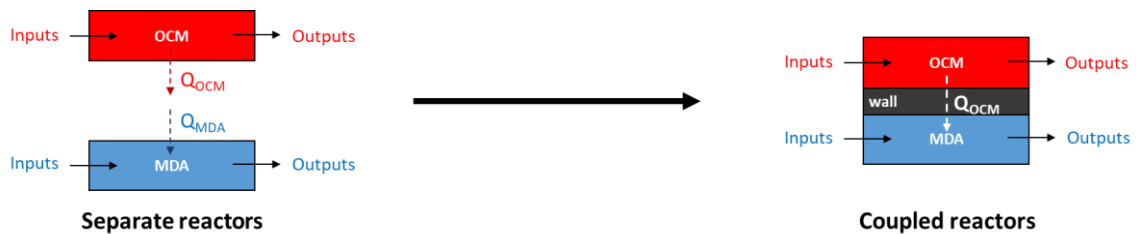


Figure V.1 Reactor design from separate reactors to coupled reactors

Before a coupled reactor design could be proposed, parameters that are critical for the reactor design will be reviewed below.

Reactor design selection, scope and targets

Reactor type selection for thermally coupled reactor is based on the degree to which heat must be removed from the reactor, as shown in the table V.2. [53]

Table V.I Reactor selection with respect to the heat of reaction

Heat of reaction	(kcal/mol product)	Reactor type
Low	<25	Fixed Bed Reactor
Moderate	50 – 120	Multi-Tubular Reactor
High	120 – 150	Fluidized Bed Reactor

Whereby,



This indicates that OCM has a moderate heat of reaction required to be removed. Hence, a multi-tubular reactor can be selected. This could either be a co-current or a counter-current design as shown in fig. V.2.

Mathematical modeling of coupled 1-D pseudo homogenous single packed bed reactor model

Schematic diagram of a thermally coupled OCM-MDA reactor, and how the reactor model was developed is shown in Figure III.1.

The following assumptions were used to build the reactor models.

1. The system is in steady state condition
2. The system is non-isothermal and non-isobaric
3. Physical properties of the catalyst are fixed
4. No heat and mass transfer limitations
5. No effect of axial dispersion

6. No heat and mass transfer with the surroundings

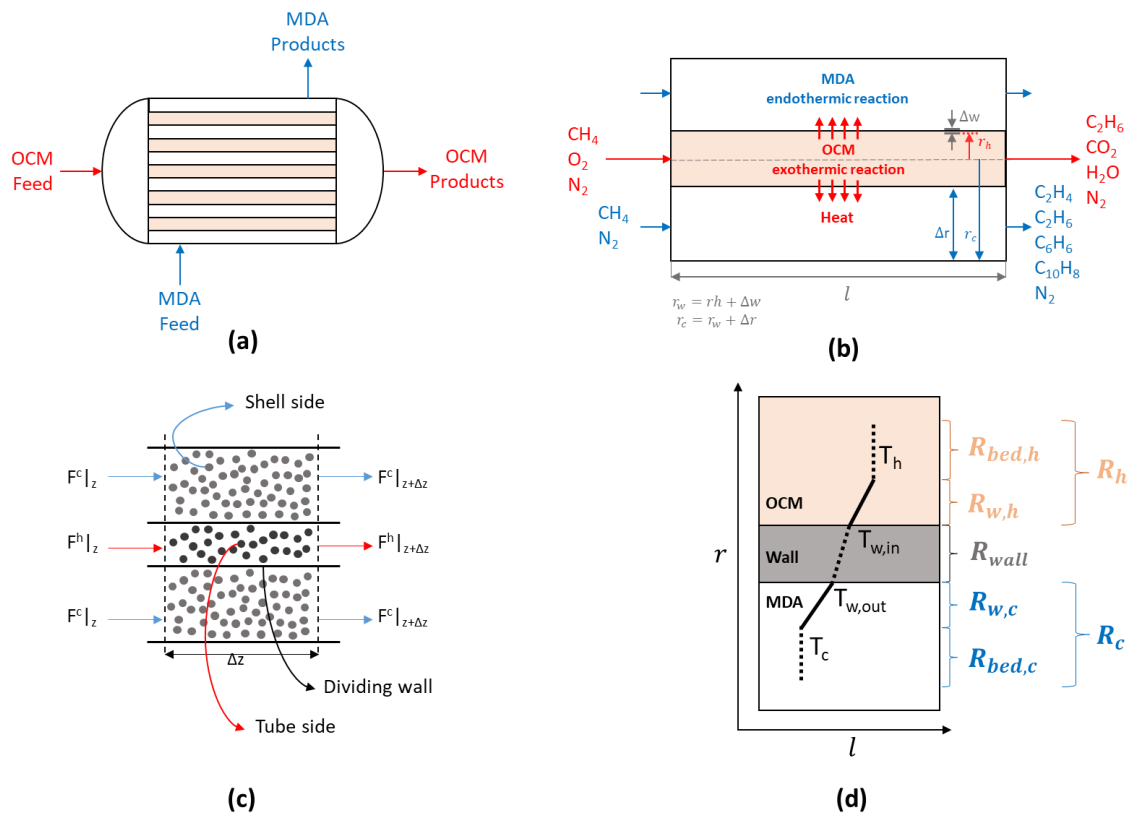


Figure V.2 Schematic diagram of thermally coupled OCM-MDA (a) multi-tubular reactor (b) single tube representation (c) elemental segment of one reactor channel (d) heat transfer resistances across the radius of reactor

Reactor design equations

Based on the reactor model assumptions and employing law of conservation of mass and energy, the following balances can be modeled:

Mole Balance:

$$\frac{\pm dF_i}{dz} = \epsilon_{cat} * A_{c,n} * r_{i,net} \quad \text{V.2}$$

$$V_{reactor} = V_{gas} + V_{catalyst} + V_{diluent} \quad \text{V.3}$$

$$\epsilon_{cat} = \frac{V_{cat}}{V_{reactor}} \quad \text{V.4}$$

Energy balance:

$$\frac{\pm dT_n}{dz} = \frac{Q_{g,n} \pm Q_{ex}}{\sum^n (F_i * C_{P_i})} \quad \text{V.5}$$

$$Q_{g,n} = \sum^n (\Delta H_{j,i} * r_{j,i}) \quad \text{V.6}$$

$$Q_{ex} = U_{overall} * 2\pi r_n * (T_h - T_c) \quad \text{V.7}$$

$$\Delta H_{j,i} = \Delta H_{j,i}^o + \Delta C_{P,j,i} (T_n - T_R) \quad \text{V.8}$$

$$\Delta H_{j,i}^o = \sum H_{f,i}^P - \sum H_{f,i}^R \quad \text{V.9}$$

$$\Delta C_{P,j,i} = \sum \left(\frac{\theta_i}{\theta_a} C_{P_i} \right)^P - \sum \left(\frac{\theta_i}{\theta_a} C_{P_i} \right)^R \quad \text{V.10}$$

The overall heat transfer coefficient was calculated by the following equation:

$$U_{overall} = \frac{1}{R_h + R_{wall} + R_c} \quad \text{V.11}$$

Where,

$$R_h = \frac{1}{\alpha_h} \quad \text{V.12}$$

$$R_{wall} = \left(\frac{\Delta w * A_h}{\lambda_w * A_m} \right) \quad \text{V.13}$$

$$R_c = \left(\frac{A_h}{A_w * \alpha_c} \right) \quad \text{V.14}$$

$$r_w = r_h + \Delta w \quad \text{V.15}$$

$$r_c = r_w + \Delta r \quad \text{V.16}$$

$$A_h = 2\pi r_h l \quad \text{V.17}$$

$$A_w = 2\pi r_w l \quad \text{V.18}$$

$$A_m = \frac{A_h - A_c}{\log \left(\frac{A_h}{A_c} \right)} \quad \text{V.19}$$

The heat transfer coefficients can be estimated using different heat transfer correlations from the literature. This will be discussed in detail in the heat transfer section of the thesis. The pressure drop across the catalyst bed length was estimated using Ergun equation. Where this equation refers specifically to tubular designs, it was used here for the annular geometry owing to its simplicity:

$$\frac{\pm dP_n}{dz} = \left(\frac{150\mu_n}{\phi_n^2 d_{p,n}^2} * \frac{(1 - \epsilon_{gas,n})^2}{\epsilon_{gas,n}^3} * \frac{Q_n}{A_{c,n}} \right) + \left(\frac{1.75\rho_n}{\phi_n d_{p,n}} * \frac{1 - \epsilon_{gas,n}}{\epsilon_{gas,n}^3} * \frac{Q_n^2}{A_{c,n}^2} \right) \quad \text{V.20}$$

Where,

$$A_{c,h} = \pi r_h^2 \quad \text{V.21}$$

$$A_{c,c} = \pi(\Delta r)^2 \quad \text{V.22}$$

The positive sign in the left-hand side of the mole balance, heat balance and pressure drop equation represents the co-current flow and negative sign for the counter-current flow reactor design. And Q_{ex} is negative for exothermic (OCM) and positive for endothermic (MDA) reaction.

Selecting acceptable ranges of reactor channels based on non-isobaric analysis of Ergun Equation

A reactor design needs to fulfill a maximum pressure drop target which depends on the reactor flow rate per channel by defining the total number of required parallel tubes, channel diameter, channel length, and catalyst particle size. Analysis of the Ergun

equation was performed to find range of acceptable reactor dimensions for a given pressure drop. For a given pressure drop per length, the maximum superficial velocity for minimum particle diameters was identified as shown in fig. V.3.

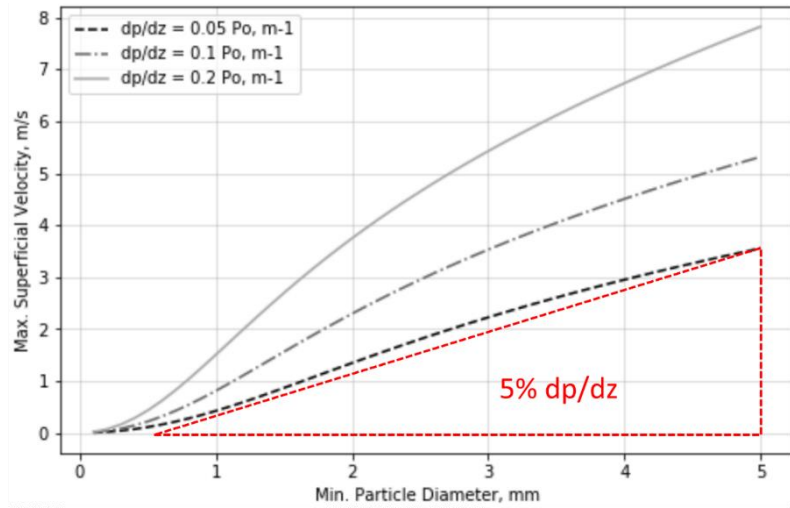


Figure V.3 Pressure drop per length for multiple pressure drops per length

For example, if the target pressure drop should be lower than 5% of dP/dz , the maximum superficial velocity is 0.2 – 3.5 m/s for a given particle diameter of 0.5 – 5 mm. Using this superficial velocity, and the reactor space velocity of 0.24 seconds, the reactor length can be found using the fig. V.4.

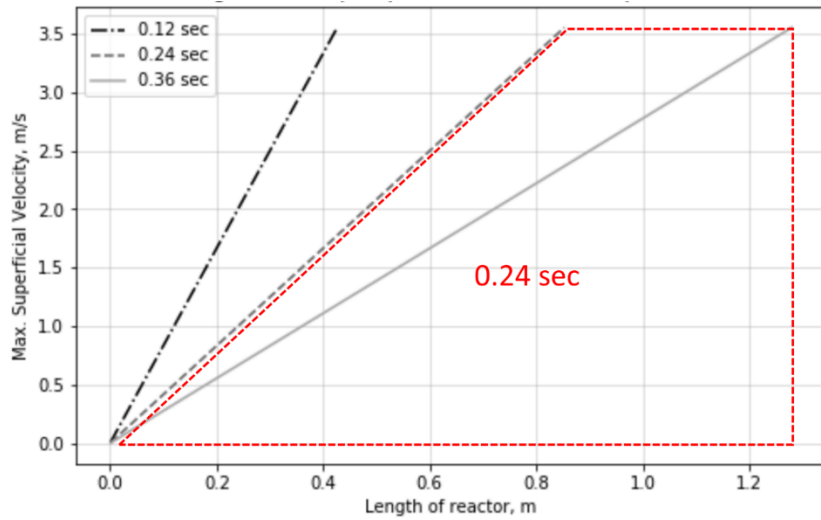


Figure V.4 Reactor length for multiple space times shown for $dp/dz = 0.05 \text{ Po m}^{-1}$

For a given space time of 0.24 seconds, 0.2 – 3.5 m/s superficial velocity corresponds to 0.05 – 0.85 m length. Based on this length, required diameter is calculated to hold catalyst weight for the given feed flowrates, e.g. for a flowrate of 10,000 the OCM catalyst required is 185 kgs.

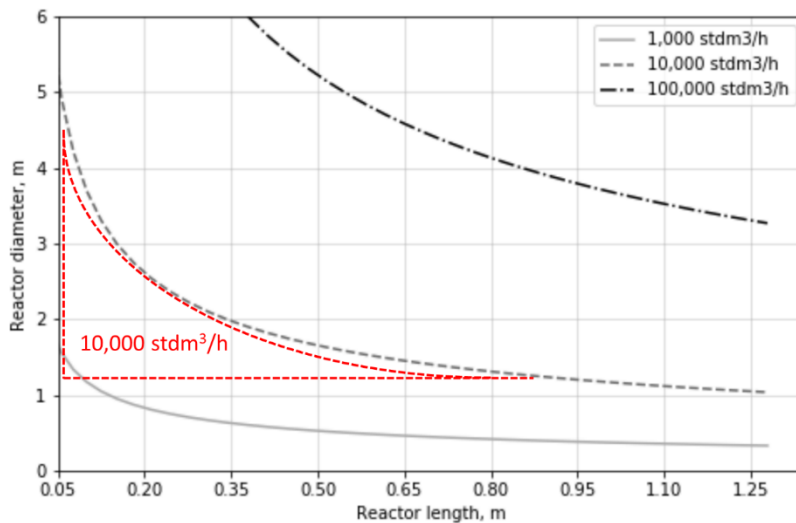


Figure V.5 Reactor dimensions for the given catalyst weight and 0.24 sec space velocity

Thus, for given 0.05 – 0.85 m length corresponds to 1.2 – 5 m total reactor dia.

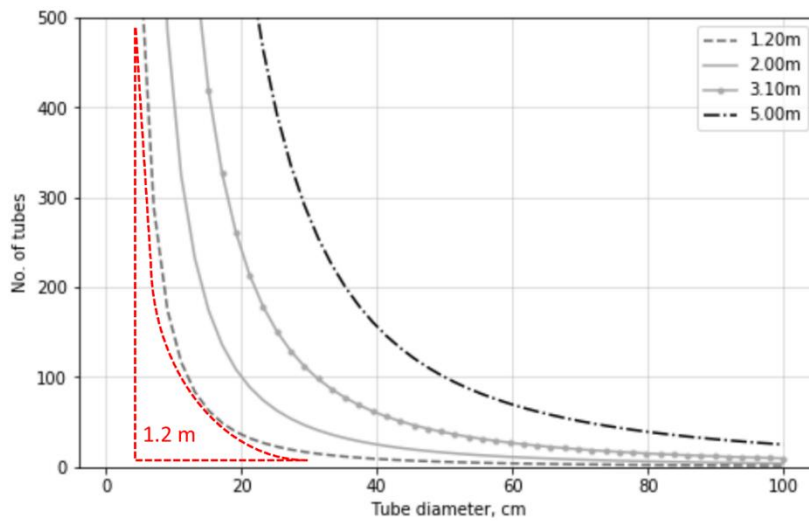


Figure V.6 Number of tubes for multiple total reactor diameters

Therefore, by choosing a reactor length from fig. V.5, the corresponding reactor diameter can be translated in the number of tubes and tube diameter e.g., 1.2 m reactor diameter has 5 to 30 cm tube diameter with 2 – 500 number of tubes required.

Therefore, such an analysis gives an initial starting point for sensible reactor dimensions.

Initial analysis of non-isothermal reactor design based on heat transfer coefficient

Overall heat transfer coefficient

Heat transfer across the reactor is mainly dictated by an overall heat transfer coefficient, U_{overall} . To identify its impact on the axial temperature profiles across the reactor bed, it was varied theoretically from a very low value of 50 to a very high value of 15000 W/m².K using the input variables shown in the table V.II:

Table V.II Input variables used for studying the effect of overall heat transfer coefficient

Cases	Operating Conditions			Feed Composition			Reactor design parameters				
	F_{total}	T_{in}	P_{in}	y_{CH_4}	y_{CH_4/O_2}	y_{inert}	L	d_{tube}	Tubes	ϵ_{gas}	$d_{part.}$
	Stdm ³ /h	°C	atm	%	-	%	cm	cm	-	%	mm
OCM	10,000	800	1	61.7	3	17.8	45	0.8	20,000	50	3
MDA	72,320	800	1	95	-	5	-	6.3	-	50	3

The aim of this analysis was to find out the minimum value which can avoid the thermal runaway and the highest value after which there remains no significant effect on the reactor performance and temperature profile.

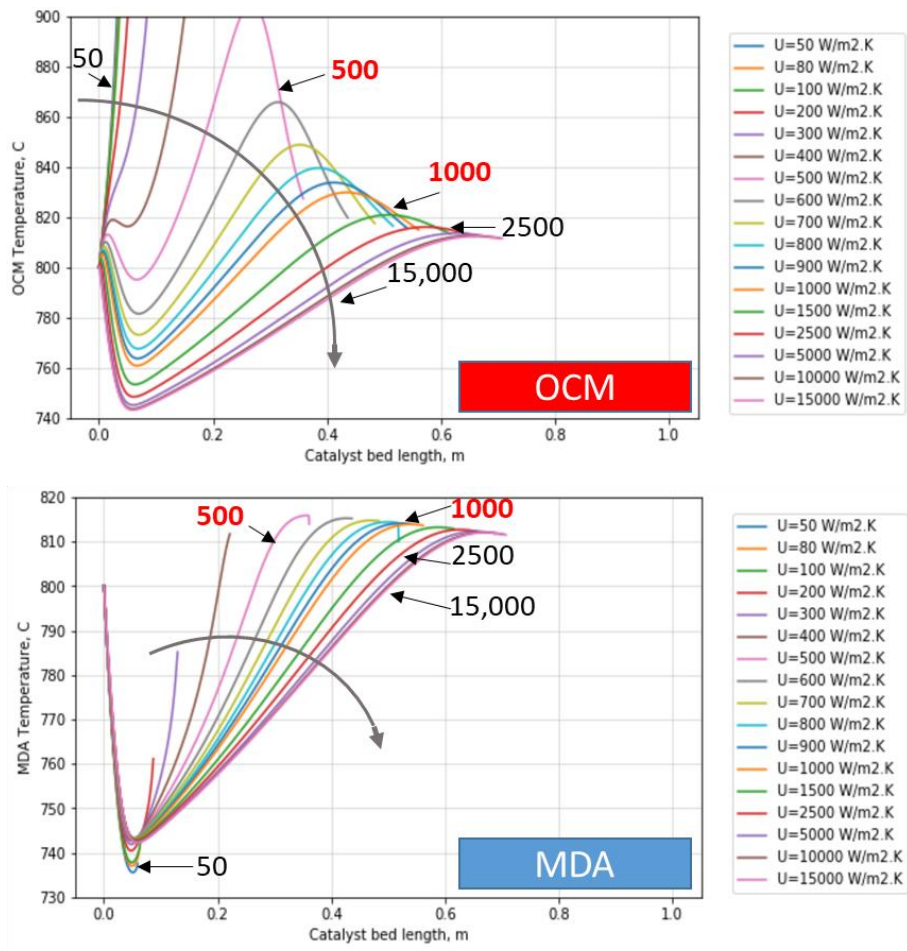


Figure V.7 OCM and MDA temperature profile along the catalyst bed for multiple values of $U_{overall}$ ranging from 50 to 15000 W/m².K

The axial temperature profiles for these values of U_{overall} are shown in Figure V.7. A minimum U_{overall} of $500 \text{ W/m}^2\cdot\text{K}$ was identified, below which a thermal runaway of $> 100 \text{ }^\circ\text{C}$ occurs and above $2500 \text{ W/m}^2\cdot\text{K}$ no significant effect on the performance and temperature profile was observed. Thus, a target value of $1000 - 2500 \text{ W/m}^2\cdot\text{K}$ is required to meet the specified design target in this case. Multiple factors can contribute to achieving this target value which will be discussed in the next section of the heat transfer models.

Predicting heat transfer coefficient from correlations in the literature

Three resistances contribute towards the U_{overall} : resistance from the OCM side, R_{OCM} ; from the wall, R_{WALL} ; and from the MDA side, R_{MDA} ; as shown in the fig. V.8.

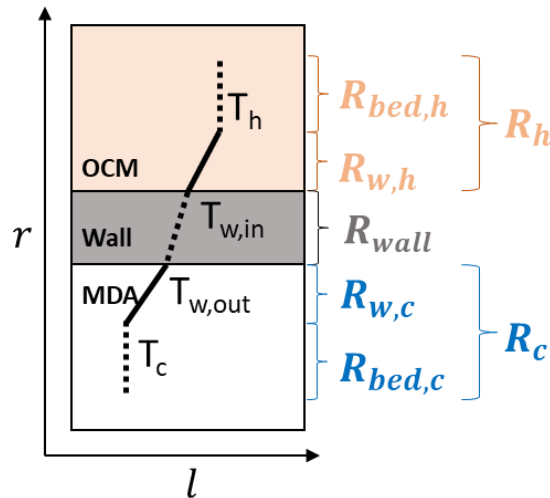


Figure V.8 Heat transfer resistances across the radius of the reactor

These resistances are calculated using the respective heat transfer coefficients, which can be predicted using different correlations from the literature, that formulate the overall heat transfer coefficient of the reactor. Generally, a heat transfer coefficient α in a

fixed bed reactor is defined by two main resistances, one α_w which is very near the wall and the other α_{bed} that is of the rest of the packed bed[54]:

$$\frac{1}{\alpha} = \frac{1}{\alpha_w} + \frac{1}{\alpha_{bed}} \quad \text{V.23}$$

To illustrate, one of the heat transfer models[54] used to predict the heat transfer coefficient is shown below:

$$\alpha_w = \alpha_w^o + \left(0.01152 Re \frac{d_t}{d_p} \right) \quad \text{V.24}$$

$$\alpha_{w,y}^o = \frac{20k_e^o}{d_t} \quad \text{V.25}$$

And,

$$\alpha_{bed} = \alpha_{bed}^o + \left(0.0025 \frac{Re}{1 + \left(46 * \frac{d_p}{d_t} \right)^2} \right) \quad \text{V.26}$$

Where,

$$\alpha_{bed}^o = k_e^o \frac{d_t^{\frac{1}{3}}}{0.42} \quad \text{V.27}$$

To understand the factors affecting the resistance, a sensitivity study was carried out.

Sensitivity study of factors affecting heat transfer coefficient

Using the heat transfer model [54], a sensitivity study was carried out to see the effect of individual parameters on the heat transfer coefficient. To do so, a reference case

with the following set of values was used and the heat transfer model was analyzed as shown in the fig. V.4.

- Tube diameter = 2 cm
- Particle diameter = 1 mm
- Superficial velocity = 0.500 m/s
- Fluid viscosity = 0.0038 Pa.s
- Fluid density = 0.19 kg/m³
- Bed conductivity = 0.37 W/m.K

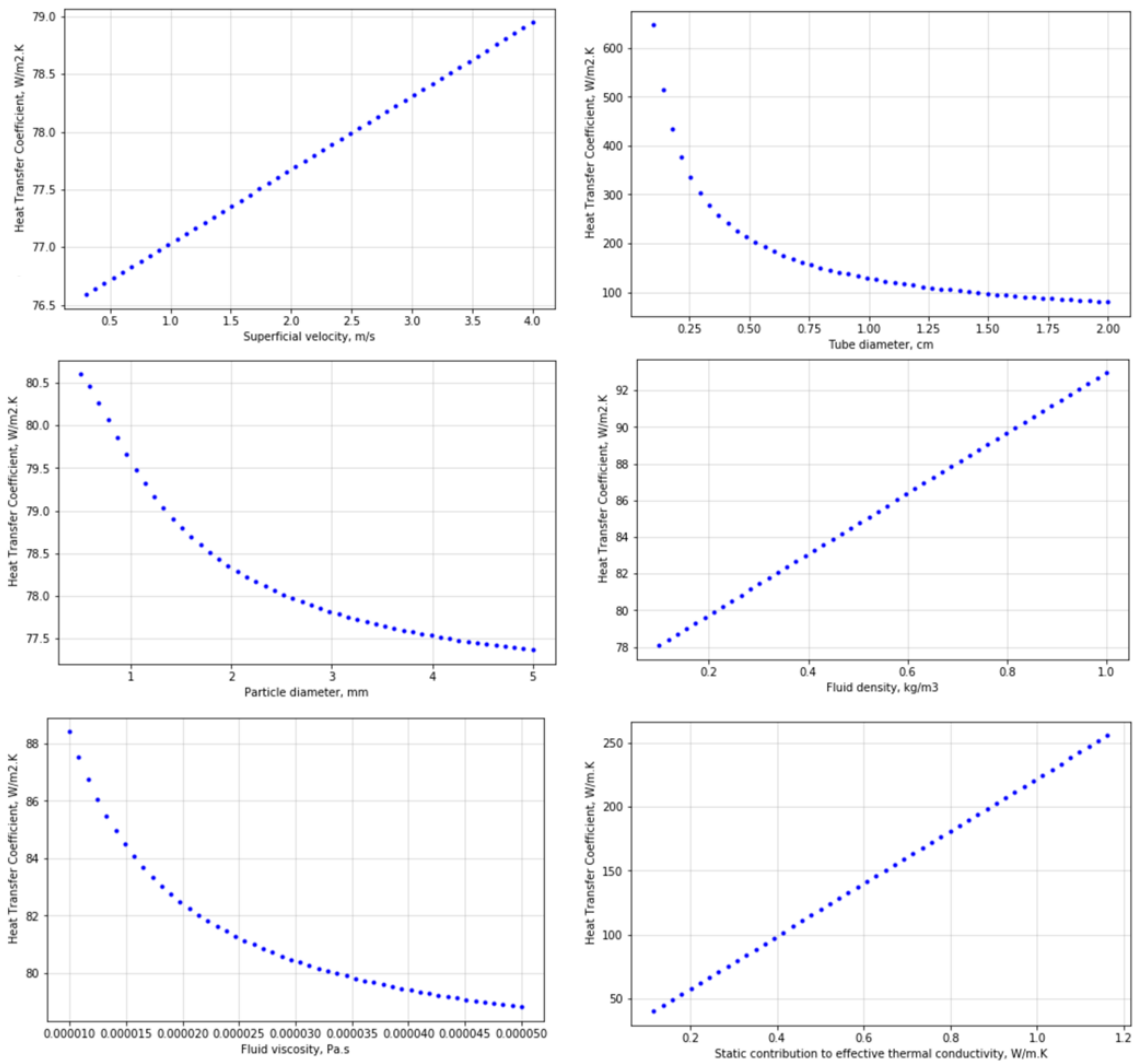


Figure V.9 Analysis of multiple parameters on the heat transfer coefficient

As shown in the fig. V.9, heat transfer coefficient can be increased by increasing superficial velocity, fluid density and bed conductivity, whereas, decreasing, tube diameter, particle diameter and fluid viscosity. The results of this heat transfer model shows that only bed conductivity has a significant impact on the heat transfer coefficient. Whereby, the superficial velocity and tube diameter shows a mild impact in this study, this is because the chosen model under the study gives a very small value of heat transfer coefficient, thereby the effect cannot be observed with signified impact.

This model provides significantly lower values of heat transfer coefficient. This might be due to the choice of a lower value of chosen bed conductivity, 0.37 W/m.K. As the bed conductivity can range from 0.7 – 8.5 W/m.K for different catalysts. [55] Another reason could be that the heat transfer model may not be suitable for our system and conditions. Thus, other heat transfer models [56]–[58] were also used to find the expected values and were compared. A summary of the values obtained by using these models is shown in table V.IV, using the conditions in table V.III:

Table V.III Input conditions used for calculating heat transfer coefficient from multiple models

Cases	Operating Conditions					Reactor design parameters					
	F_{total} Stdm ³ /h	T_{in} °C	P_{in} atm	Feed	V_s m/s	L cm	d_{tube} cm	Tubes -	ϵ_{gas} %	$d_{part.}$ mm	λ_{pellet} W/m.K
OCM	10,000	800	1	CH ₄	2.6	100	0.8	20,000	50	3	1.2
MDA	72,320	800	1	CH ₄	0.5	-	6.3	-	50	3	1.2

Table V.IV Predicted heat transfer coefficients from multiple correlations from the literature

Model	h_{OCM} (W/m ² .K)	h_{MDA} (W/m ² .K)	$U_{overall}$ (W/m ² .K)
Leva, 1950 [56]	44	3	4
De Wasch & Froment, 1972 [54]	160	123	88
Dixon and Cresswell, 1979 [57]	263	382	182
Tsotsas & Schlünder, 1990 [58]	945	163	203

In the table V.IV, all the values of $U_{overall}$ show a large deviation using different models. This causes a difficulty in choosing the right model to choose. Also, all the values of $U_{overall}$ obtained are very low (< 200 W/m².K) as compared to the targeted values of $1000 - 2500$ W/m².K as discussed in the analysis section of overall heat transfer coefficient. This indicates that the chosen design for calculating this heat transfer coefficient is not appropriate and thereby the design needs to be changed. The large variance in the results also indicate that further studies are required in performing experimentations for building precise heat transfer models.

Further analyzing the results also indicate that the heat transfer coefficient of the MDA side is lowest, representing that MDA side is heat transfer rate limiting and thus resistance from MDA needs to be decreased in order to increase the value of overall heat transfer coefficient. Which can be done by increasing the thermal conductivity of the bed and the superficial velocity of the MDA side, as discussed in the analysis section of heat transfer coefficient.

**Altering the axial temperature profile to acceptable design targets via catalyst
profiling and diluents**

Effect of diluents on temperature profile

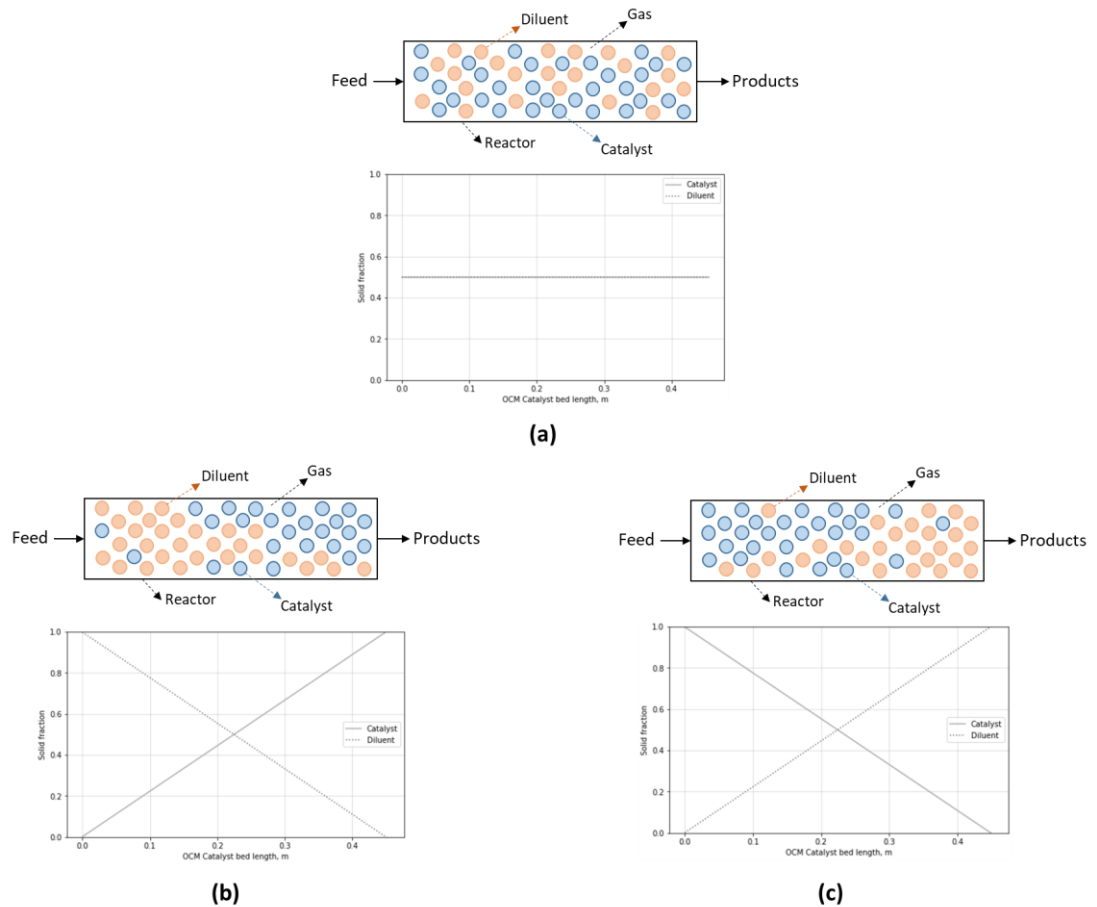


Figure V.10 Schematic diagram of a reactor with homogeneously packed catalyst with diluents (a); Two different ways of catalyst profiling (b & c)

In this work, diluents are assumed to be particles having the same physical properties as that of the catalysts but are catalytically inactive. These are added to the catalyst bed to control the heat transfer distribution, and thus the temperature profile of the reactor. It is also assumed that the gas void fraction remains constant at 0.5.

To analyze the effect on the temperature profile, diluents were added in OCM reaction channels such that the geometrical dimensions of reaction channels remained the same as 0.8 cm tube diameter and 1 m length. However, adding diluent had caused the reactor volume to increase, thus was accommodated by increasing the number of parallel tubes in the multi-tubular reactor as needed. The inputs used in this study are summarized in the table V.V.

Table V.V Input variables used for studying the effect of diluents on the temperature profile

Cases	Operating Conditions			Feed Composition			Reactor design parameters			
	F_{total}	T_{in}	P_{in}	Y_{CH_4}	Y_{CH_4/O_2}	Y_{inert}	L	d_{tube}	ϵ_{gas}	$d_{part.}$
	Stdm ³ /h	°C	atm	%	-	%	cm	cm	%	mm
OCM	10,000	800	1	61.7	3	17.8	100	0.8	50	3
MDA	72,320	800	1	95	-	5	-	6.3	50	3

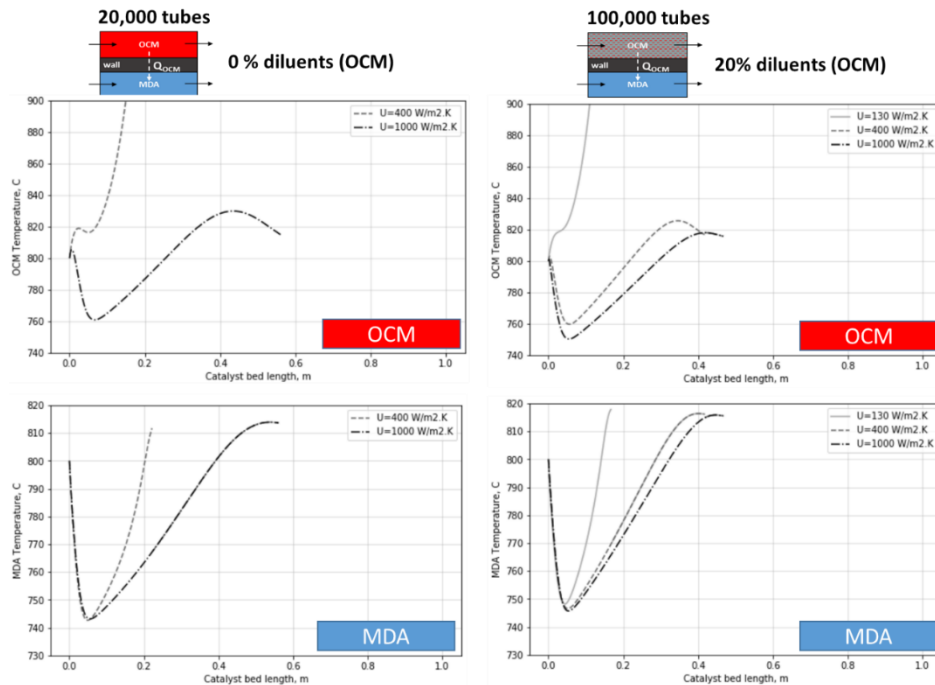


Figure V.11 Effect of adding diluents on the temperature profiles of an OCM-MDA reactor with 0% diluents and $U_{overall} = 400$ and $1000 \text{ W/m}^2.\text{K}$ (left) and 40% diluents with $U_{overall} = 130, 400$ and $1000 \text{ W/m}^2.\text{K}$ (right)

Figure V.11 shows the temperature profiles for OCM and MDA for two cases with diluents and without diluents. As the diluents are increased from 0 to 40%, the thermal runaway does not happen and the profiles tends to be closer to that of the higher heat transfer coefficients, thereby, heat transfer limitation is decreased. Whereas, to achieve the same thermal runaway with diluents, a lower U_{overall} of $130 \text{ W/m}^2\cdot\text{K}$ is required. Thus, adding diluents helps in decreasing the requirements of having a higher heat transfer coefficient and avoids thermal runaway. However, the size of the reactor volume is increased to accommodate the added diluents.

Effect of OCM catalyst profiling for a fixed catalyst and diluent void fraction

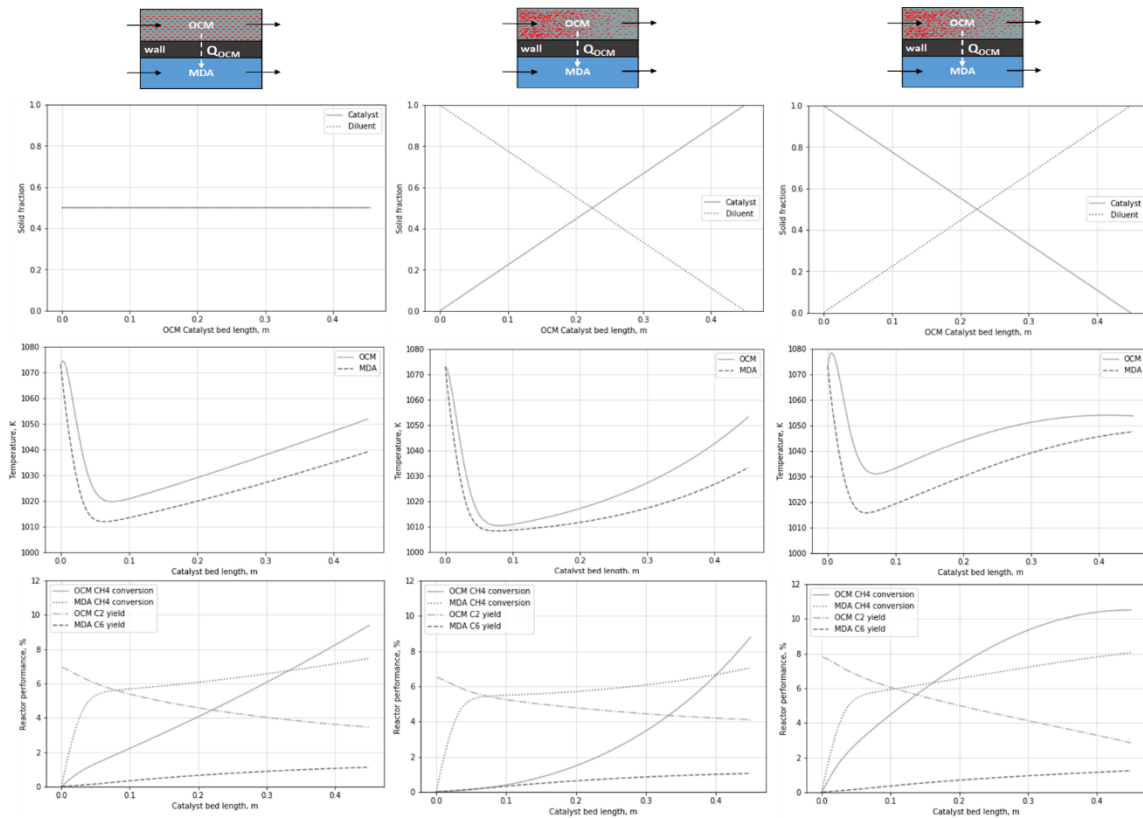


Figure V.12 Catalyst profiling, temperature profiles and reactor performance of the OCM-MDA reactor for 50% gas volume, 0% MDA diluent and OCM 50%

homogenous diluent (left), 100 to 0% diluent profiling (middle) and 0 to 100% diluent profiling (right)

Table V.VI Input variables for studying the effect of OCM catalyst profiling

Cases	Operating Conditions				Feed Composition			Reactor design parameters					
	F_{total}	T_{in}	P_{in}	Sp. Time	y_{CH_4}	y_{CH_4/O_2}	y_{inert}	L	d_{tube}	Tubes	$U_{overall}$	ϵ_{gas}	$d_{part.}$
	Stdm ³ /h	°C	atm	sec	%	-	%	cm	cm	-	W/m ² .K	%	mm
OCM	10,000	800	1	0.4	61.7	3	17.8	45	0.8	20000	1000	50	3
MDA	72,320	800	1	2	95	-	5	-	6.3	-	-	50	3

Figure V.12 compares 50% homogenous OCM diluents with a mixing case of 100% to 0% and 0% to 100% diluents, for the input variables shown in table V.VI. Increasing OCM diluents along the bed avoids thermal runaway as it lowers the exothermic reaction rate. Whereas profiling affects axial temperature profile in this case, but within 10 degrees. For different conditions and starting points, this technique might be a good way to control temperature profile.

Effect of MDA catalyst profiling for a fixed catalyst and diluent void fraction

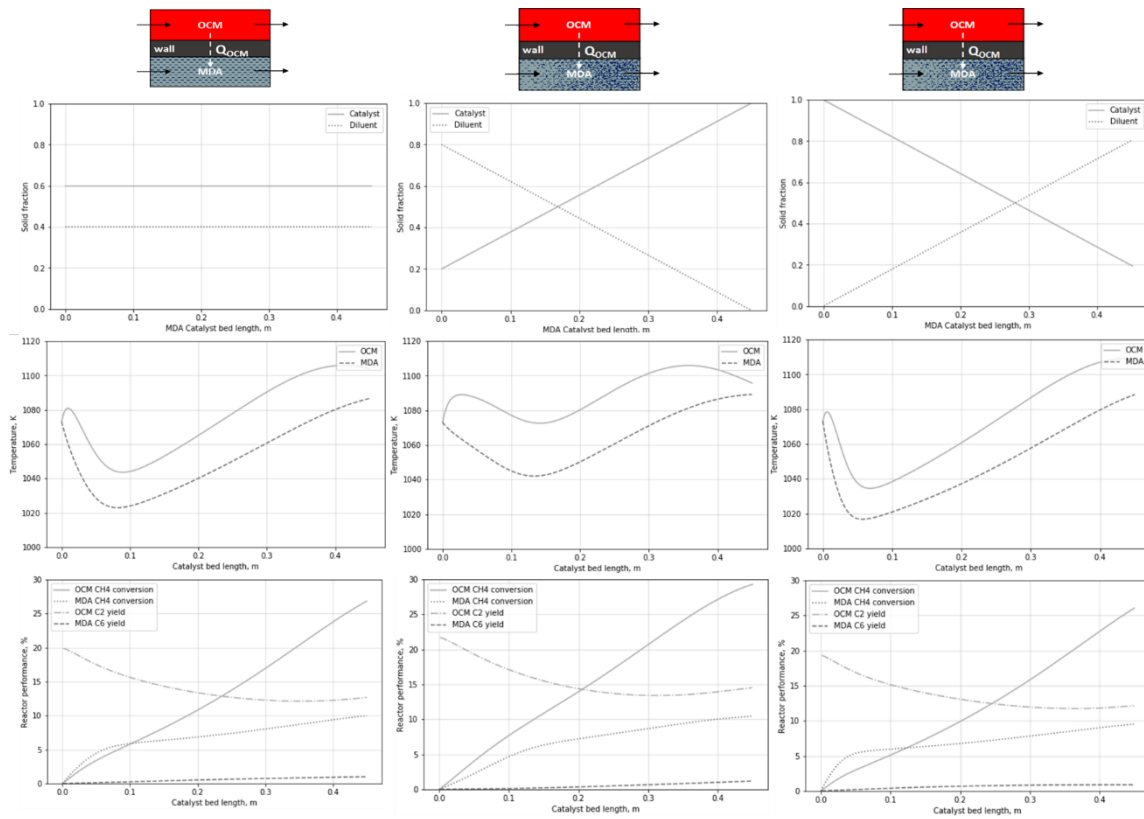


Figure V.13 Catalyst profiling, temperature profiles and reactor performance of the OCM-MDA reactor for 50% gas volume, 0% OCM diluent and MDA 40% homogenous diluents (left), 80 to 0% diluent profiling (middle) and 0 to 80% diluent profiling (right)

Table V.VII Input variables for studying the effect of MDA catalyst profiling

Cases	Operating Conditions				Feed Composition			Reactor design parameters					
	F_{total}	T_{in}	P_{in}	Sp. Time	Y_{CH_4}	Y_{CH_4/O_2}	Y_{inert}	L	d_{tube}	Tubes	$U_{overall}$	ϵ_{gas}	$d_{part.}$
	Stdm ³ /h	°C	atm	sec	%	-	%	cm	cm	-	W/m ² .K	%	mm
OCM	10,000	800	1	0.4	61.7	3	17.8	45	0.8	20000	1000	50	3
MDA	72,320	800	1	2	95	-	5	-	6.3	-	-	50	3

Figure V.13 compares 40% homogenous MDA diluents with a mixing case of 80% to 0% and 0% to 80% diluents, for the input variables shown in table V.VII. More diluents at the start of MDA reactor can lower the initial endothermic reaction rate, avoid the MDA temperature dip at the reactor start. The catalyst profiling affects axial temperature profile

in this case, but within 10 degrees, however, there is a limit to which we can lower the MDA diluents at the reactor inlet as further diluents lowering causes OCM thermal runaway.

Co-current versus counter-current flow direction analysis

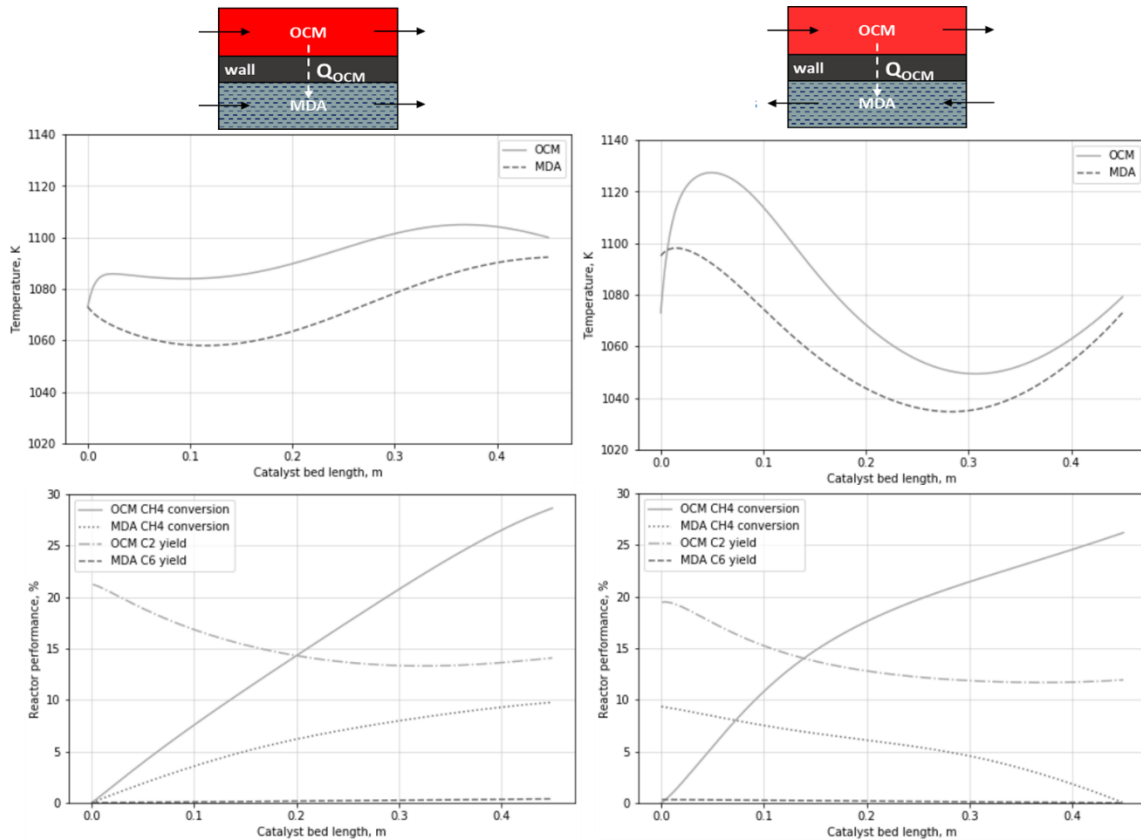


Figure V.14 Comparison of a co- (left) and counter-current (right) reactor temperature and performance profiles

Table V.VIII Input variables for studying the effect of co-current and counter-current reactor designs

Cases	Operating Conditions				Feed Composition			Reactor design parameters						
	F_{total} Std m^3/h	T_{in} $^{\circ}C$	P_{in} atm	Sp. Time sec	y_{CH_4} %	y_{CH_4/O_2} -	y_{inert} %	L cm	d_{tube} cm	Tubes -	$U_{overall}$ W/ $m^2.K$	ϵ_{gas} %	$\epsilon_{diluent}$ %	$d_{part.}$ mm
OCM	10,000	800	1	0.4	61.7	3	17.8	45	0.8	20,000	1000	50	0	1
MDA	72,320	800	1	2	95	-	5	-	6.3	-	-	50	80	1

Fig. V.14 represents a comparison between a co- and a counter-current reactor for 0% OCM diluents and 20% MDA diluents for the input variables shown in table V.VIII. This shows that the choice of a counter-current design allows for a better temperature control, but not for higher reactor performances. A counter-current design allows for tweaking the temperature profiles, which also impacts the reactor performance profiles of both, OCM and MDA. Unlike the co-current case, the counter-current design shows a decrease in the reactor performance towards the end of the reactor. This is because the fresh feed of MDA enters from the end of the reactor and quenches the heat, thereby, reducing the OCM temperature and thus OCM performance. The same phenomenon can be observed at the start of the reactor, whereby fresh OCM feed enters, and thus there is a temperature peak which is observed which also causes a rise in OCM reactor performance.

Guidelines for approaching an isothermal reactor temperature and performance

Based on the above studies of diluents, catalyst profiling and flow direction, it can be concluded that:

1. Counter-current can help to control the reactor temperature profile significantly, but also has a slight impact on the reactor performance.
2. More diluents at the start of MDA reactor can lower the initial endothermic reaction rate, avoid the MDA temperature dip at the reactor start and thus, flatten the temperature profile.
3. For a counter-current design, lesser diluents at the end of the MDA reactor will allow for higher endothermic reaction at the reactor end, which will help in quenching the high inlet heat of OCM reaction, thus flatten the OCM temperature peak.

- Increasing OCM diluents along the bed avoids thermal runaway as it lowers the exothermic reaction rate.
- Higher value of $U_{overall}$ with no diluents, or, lower value of $U_{overall}$ but with diluents, removes the heat transfer limitation and approaches the isothermal reactor performance profile.

Thermal coupling optimization of showcase coupled reactors using neural network

Based on the design targets and other parameters, like $U_{overall}$, diluents, catalyst profiling and flow direction, a coupled case can be designed while using separate coupling case as a starting point shown in table V.IX.

Table V.IX Base case taken from separate reactors for coupled reactors study

Cases	Operating Conditions				Feed Composition				Reactor Performance			Heat & Cat. Wt.		
	F	T	P	GHSV	Y_{CH_4}	Y_{CH_4/O_2}	Y_{inert}	Y_{C_2/C_6}	X_{CH_4}	X_{O_2}	S_{C_2/C_6}	Q	m_{Cat}	Cat R MDA/OCM
	Stdm ³ /h	°C	atm	h ⁻¹	%	-	%	%	%	%	%	MW	tons	-
OCM (Ref. Case)	10,000	800	1	14,919	61.7	3	17.8	33.8	46.1	99.99	73.2	9.95	0.18	54.1
MDA (Opt. Case)	72,320	800	1	3,688	95	-	5	0.95	12.3	-	7.6	9.95	10	-

This case was used as a reference case along with the constraints obtained from the coupled reactor case studies. A single-variable-at-a-time optimization was then performed to achieve a coupled reactor design shown in the fig. V.15, using the following design targets:

- Maximum pressure drop is 20% of inlet pressure
- Maximum variation along the axial temperature profile (T_{peak} or T_{lower}) needs to be lower than 100 °C
- OCM C_2 yield is at least 30%
- MDA CH_4 conversion is at least 10%

Input Layer					OCM-MDA Reactor			Output Layer				
Opt. Priority	Name	Units	Initial Value	Constraints	Optimizer	Optimized Value	Reactor Model	Name	Units	Initial Value	Opt. Value	Target
1	Inlet Temperature	C	800	800		800	OCM	C ₂ Yield	%	10.1	30.1	> 30
2	Inlet Pressure	atm	1	1		1		CH ₄ Conv.	%	22.5	42.9	
3	Feed flow rate	Std ³ /h	10,000	10,000		10,000		O ₂ Conv.	%	81.7	99.4	
4	Feed composition (CH ₄)	%	61.7	61.7		61.7		Re. No. for particle	-	13.3	39.9	
5	Feed composition (Inerts)	%	17.8	17.8		17.8		ΔP (% of Pin)	%	19	2.8	<20
6	Superficial velocity	m/s	2.6	0.2–3.5		2.6		T _{peak} (T _{max} – T _{in})	K	21.9	97.0	<100
7	Particle dia.	mm	1	0.5–5.0		3.0		T _{lowest} (T _{in} – T _{min})	K	39.7	0.0	
8	Tube dia.	cm	0.8	0.5–10.0		1.7		σT	K	19.8	21.7	
9	Gas void fraction	-	0.5	0.5		0.5		Space time	sec	0.4	0.4	
10	Catalyst void fraction	-	0.5	0.01–0.5		0.5		Catalyst weight	kgs	83.25	74	
11	Flow direction	Co-current		Co-/Counter-		Co-current		U _{overall}	W/m ² .K	1000	1000	1000-2500
12	Channel length	cm	45	5–85	Optimizer	40		No. of tubes	-	20000	5000	
13	Tube wall thickness	mm	5	2–20		5						
14	Inlet Temperature	C	800	800		800	MDA	C ₂ Yield	%	1.4	0.3	
15	Inlet Pressure	atm	1	1		1		CH ₄ Conv.	%	9.6	10.0	10
16	Feed flow rate	Std ³ /h	72,320	72,320		72,320		Re. No. for particle	-	14.2	8.9	
17	Feed composition (Inerts)	%	5	5		5		ΔP (% of Pin)	%	2.1	0.2	<20
18	Superficial velocity	m/s	0.5	0.2–3.5		0.5		T _{peak} (T _{max} – T _{in})	K	1.2	19.9	
19	Particle dia.	mm	1.0	0.5–5.0		3.0		T _{lowest} (T _{in} – T _{min})	K	56.9	17.8	< 100
20	Tube dia.	cm	5.0	0.5–10.0		10.0		σT	K	18.1	13.8	
21	Gas void fraction	-	0.5	0.5		0.5		Space time	sec	2.0	2.0	
22	Catalyst void fraction	-	0.5	0.1–0.5		0.1		Catalyst weight	kgs	4500	4000	

Figure V.15 Final results of reactors coupling methodology

This design was developed with 5000 total tubes, an OCM tube diameter of 1.7 cm with 0.07 tons of catalyst, MDA tube diameter of 11.2 cm with 4 tons of catalyst and a reactor length of 40 cm, as shown in the fig. V.16.

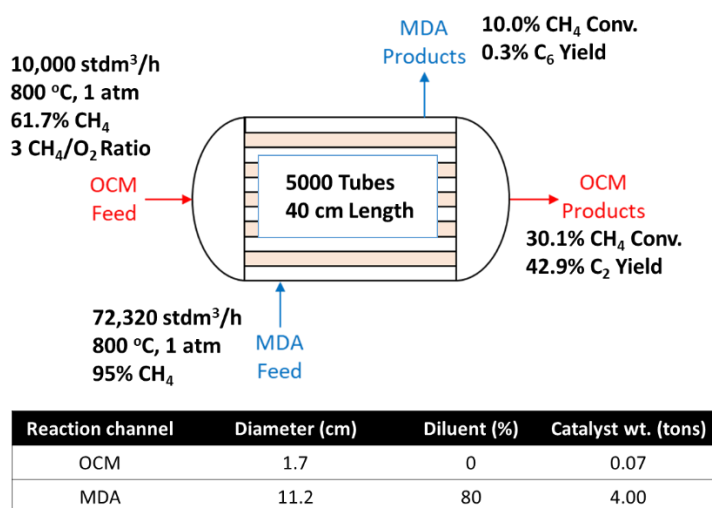


Figure V.16 Showcase of an autothermal reactor design

The reactor temperature profile and performance is shown fig. V.12.

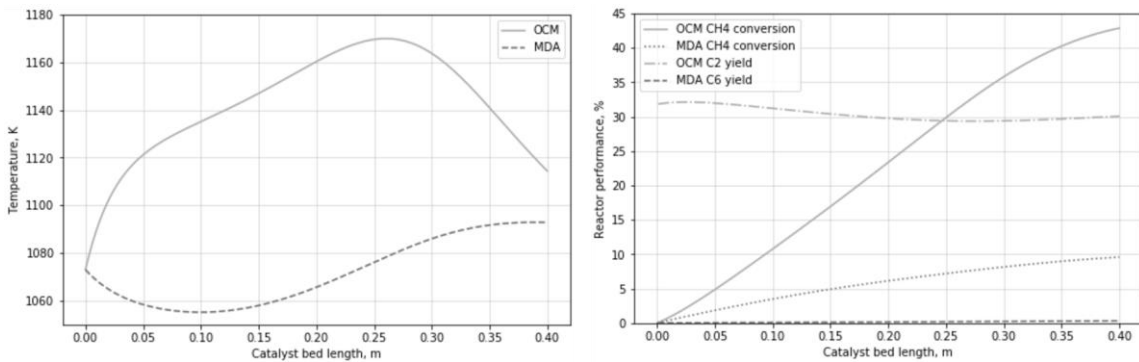


Figure V.17 Coupled reactor temperature profile (left) and performance along the catalyst bed (right)

Further showcases of acceptable autothermal reactor designs can be built for the same input conditions yet different reactor dimensions shown in fig. V.18.

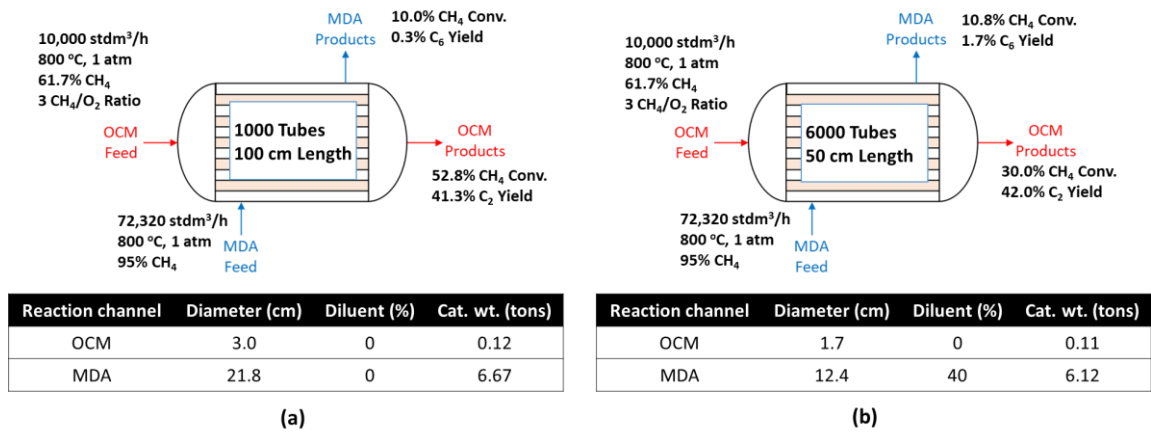


Figure V.18 Showcase of other acceptable autothermal reactor designs

CHAPTER VI

CONCLUSIONS

Direct conversion processes like OCM and MDA have their own challenges, however, based on the current study of separate reactors, thermal coupling can be achieved within an operating range of 700 – 800 °C temperature and 1 – 5 atm pressure with GHSV 830 – 14,000 h⁻¹ with heat duties of 1 MW to 13 MW. Hereby, a structured approach has been established which can assist in coupling the two processes in a single reactor. This methodology can incorporate practical constraints like reactor sizing, costs, and environmental constraints by taking logical assumptions and can be utilized for any other processes than OCM-MDA. It provides a good estimate and a thorough understanding of how actual thermal coupling of reactors may be done. After the initial separate reactors coupling, work has been carried out on coupled reactors coupling by studying various parameters like heat transfer coefficient, diluents, catalyst profiling and flow direction.

Furthermore, since a large variance is seen in the results of heat transfer models for calculating the heat transfer coefficients, it is required to further study on achieving the heat transfer coefficient more precisely. Thus, further experimental studies are required in this field. After which possible reactor designs should then be studied for achieving the target overall heat transfer coefficient between 1000-2500 W/m².K whereby the system is no more limited by the heat transfer. Also, since this study utilizes a lumped value overall heat transfer coefficient, the effect of different values of individual heat transfer coefficients of OCM and MDA can significantly impact the reactors temperature

profiles of owing to the reactor's geometry. Such a study can be performed using computational fluid dynamics.

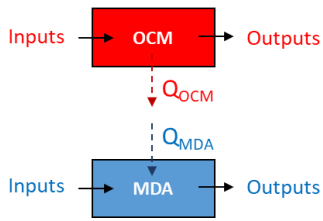
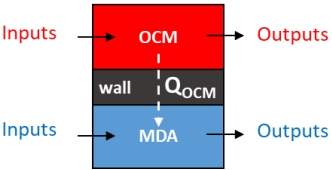
Furthermore, with the current fixed bed reactor design for OCM side, multiple fresh oxygen feed injections can be utilized for higher methane conversion. Other reactor types, such as fluidized bed reactor design can also be explored for better temperature control, and membrane type reactors for achieving higher product selectivity. In specific, MDA yield should be improved from an industrial point of view when proposing a coupled reactor. Also, catalyst deactivation plays a huge role in MDA process, thus, its impact needs to be studied on how it can affect the reactors coupling and temperature profile. Another factor that could be utilized for controlling the reactor temperature is optimization of the catalyst shape in terms of its active surface area.

An important aspect of this study is that it is based on chosen global kinetic models that were utilized to establish a coupling methodology and studies have been performed beyond their validity ranges. Thus, the results can be significantly affected while using another global kinetic model. And much more details can be further exploited by using microkinetic models. Such models are readily available in the literature and can be referred in the literature section of this thesis.

Moreover, the single-variable-at-time optimization approach used in this work results in achieving local optima and thereby different solutions, depending on the initial conditions, can be formulated. Therefore, there is a definite scope and a requirement for working towards achieving a global optimum. Such a work can be done using multi-variable optimization starting with separate reactors and then towards dependent reactors,

as shown in the table VI.I. By achieving the multivariable optimization of coupled reactors, a solution towards actual coupling of these reactors can be found and such a learning can be implemented in real world case studies such as in laboratories to understand the processes for scalability purposes.

Table VI.I Current status and future work for the optimization of reactors

OCM-MDA reactors thermal coupling	<p style="text-align: center;">Independent Reactors</p> 	<p style="text-align: center;">Dependent Reactors</p> 
<p>Single-variable optimization <i>(Manual process)</i></p>	<ul style="list-style-type: none"> • Starting point for thermal coupling • Isothermal & Isobaric Reactors • Local optima limitation 	<ul style="list-style-type: none"> • Thermal coupling design in single reactor • Non-isothermal & non-isobaric Reactors • Heat transfer through wall
<p>Multi-variable optimization <i>(Automated process)</i></p>	<ul style="list-style-type: none"> • Step towards finding global optimum • Isothermal & Isobaric Reactors • Quick solutions for decision making 	<ul style="list-style-type: none"> • Practical single reactor design • Non-isothermal & non-isobaric Reactors • Reliable engineered results for decisions

It is also important to take note of the intrinsic challenges of OCM and MDA challenges and find solutions separately for these processes prior to coupling them in a single system and scaling up to an industrial level for commerciality purposes. As such, OCM, is very exothermic and thus safety management systems capable of protecting from overheating are required. At the same time, MDA has an intrinsic challenge of rapid coking and thus continuous regeneration is required for the reactor operation. Such known

challenges are required to be solved individually, as these could not only complicate the reactor design and but also make the operations hard in terms of monitoring and control, and safety.

Nonetheless, this study paves path and establishes a good basis upon which any exo- and an endo-thermic reaction system can be coupled, in general, and OCM and MDA, in specific. The conclusions can further be taken as a basis to study further and perform laboratory experimentations that consider realistic challenges like safety and improving reactor performances.

REFERENCES

- [1] H. Ritchie and M. Roser, “Emissions by sector,” 2020. [Online]. Available: <https://ourworldindata.org/emissions-by-sector>. [Accessed: 24-Mar-2021].
- [2] L. Chen, Z. Qi, S. Zhang, J. Su, and G. A. Somorjai, “Catalytic hydrogen production from methane: A review on recent progress and prospect,” *Catalysts*, vol. 10, no. 8, 2020.
- [3] C. Karakaya and R. J. Kee, “Progress in the direct catalytic conversion of methane to fuels and chemicals,” *Prog. Energy Combust. Sci.*, vol. 55, pp. 60–97, 2016.
- [4] U. Zavyalova, M. Holena, R. Schlögl, and M. Baerns, “Statistical analysis of past catalytic data on oxidative methane coupling for new insights into the composition of high-performance catalysts,” *ChemCatChem*, vol. 3, no. 12, pp. 1935–1947, 2011.
- [5] A. Galadima and O. Muraza, “Advances in Catalyst Design for the Conversion of Methane to Aromatics: A Critical Review,” *Catal. Surv. from Asia*, vol. 23, no. 3, pp. 149–170, 2019.
- [6] G. E. Keller and M. M. Bhasin, “Synthesis of ethylene via oxidative coupling of methane. I. Determination of active catalysts,” *J. Catal.*, vol. 73, no. 1, pp. 9–19, 1982.
- [7] Z.-G. Zhang, “Process, reactor and catalyst design: Towards application of direct conversion of methane to aromatics under nonoxidative conditions,” *Carbon Resour. Convers.*, vol. 2, no. 3, pp. 157–174, 2019.
- [8] V. T. Amorebieta and A. J. Colussi, “Kinetics and mechanism of the catalytic

- oxidation of methane over lithium-promoted magnesium oxide,” *J. Phys. Chem.*, vol. 92, no. 16, pp. 4576–4578, 1988.
- [9] J. M. Deboy and R. F. Hicks, “Kinetics of the Oxidative Coupling of Methane over 1 wt% Sr/La₂O₃,” 1988.
- [10] E. Iwamatsu and K. I. Aika, “Kinetic analysis of the oxidative coupling of methane over Na⁺-doped MgO,” *J. Catal.*, vol. 117, no. 2, pp. 416–431, 1989.
- [11] J. A. Roos, S. J. Korf, R. H. J. Veehof, J. G. van Ommen, and J. R. H. Ross, “Kinetic and mechanistic aspects of the oxidative coupling of methane over a Li/MgO catalyst,” *Appl. Catal.*, vol. 52, no. 1, pp. 131–145, 1989.
- [12] E. E. Miro, J. M. Santamaria, and E. E. Wolf, “Oxidative coupling of methane on alkali metal-promoted nickel titanate. II. Kinetic studies,” *J. Catal.*, vol. 124, no. 2, pp. 465–476, 1990.
- [13] H. Zanthoff and M. Baerns, “Oxidative Coupling of Methane in the Gas Phase. Kinetic Simulation and Experimental Verification,” *Ind. Eng. Chem. Res.*, vol. 29, no. 1, pp. 2–10, 1990.
- [14] Y. Feng, J. Niiranen, and D. Gutman, “Kinetic studies of the catalytic oxidation of methane. 2. Methyl radical recombination and ethane formation over 1 % Sr/La₂O₃,” *J. Phys. Chem.*, vol. 95, no. 17, pp. 6564–6568, 1991.
- [15] L. Lehmann and M. Baerns, “Kinetic Studies of the Oxidative Coupling of Methane over a NaOH/CaO Catalyst,” *Stud. Surf. Sci. Catal.*, 1992.
- [16] S. C. Reyes, E. Iglesia, and C. P. Kelkar, “Kinetic-transport models of bimodal reaction sequences-I. Homogeneous and heterogeneous pathways in oxidative

- coupling of methane,” *Chem. Eng. Sci.*, vol. 48, no. 14, pp. 2643–2661, 1993.
- [17] S. Cheng and X. Shuai, “Simulation of a catalytic membrane reactor for oxidative coupling of Methane,” *AIChE J.*, vol. 41, no. 6, pp. 1598–1601, 1995.
- [18] W. Wang and Y. S. Lin, “Analysis of oxidative coupling of methane in dense oxide membrane reactors,” *J. Memb. Sci.*, 1995.
- [19] U. Pannek and L. Mleczko, “Comprehensive model of oxidative coupling of methane in a fluidized-bed reactor,” *Chem. Eng. Sci.*, vol. 51, no. 14, pp. 3575–3590, 1996.
- [20] M. Sohrabi, B. Dabir, A. Eskandari, and R. D. Golpasha, “Some aspects of kinetics and mechanism of the oxidative coupling of methane,” *J. Chem. Technol. Biotechnol.*, vol. 67, no. 1, pp. 15–20, 1996.
- [21] Z. Stansch, L. Mleczko M, and Baerns, “Comprehensive Kinetics of Oxidative Coupling of Methane over the La₂O₃/CaO Catalyst,” *Ind. Eng. Chem. Res.*, vol. 36, no. 7, pp. 2568–2579, 1997.
- [22] Y. I. Pyatnitsky, N. I. Ilchenko, and M. V. Pavlenko, “Kinetic aspects of the methane oxidative coupling at elevated pressures,” *Catal. Today*, vol. 42, no. 3, pp. 233–240, 1998.
- [23] M. Traykova, N. Davidova, J. Tsaih, and A. H. Weiss, “Oxidative coupling of methane ± the transition from reaction to transport control over La₂O₃ / MgO catalyst,” vol. 169, pp. 237–247, 1998.
- [24] N. S. Matin and R. Ahmadi, “Kinetics of oxidative coupling of methane over Na/BaTiO₃/MgO catalyst: Mechanistic aspects,” *J. Japan Pet. Inst.*, vol. 49, no. 1,

- pp. 13–21, 2006.
- [25] J. A. Langille, J. Pasale, J. Y. Ren, F. N. Egolfopoulos, and T. T. Tsotsis, “The use of OCM reactors for ignition enhancement of natural gas combustion for practical applications: Reactor design aspects,” *Chem. Eng. Sci.*, vol. 61, no. 20, pp. 6637–6645, 2006.
- [26] J. Sun, J. W. Thybaut, and G. B. Marin, “Microkinetics of methane oxidative coupling,” *Catal. Today*, vol. 137, no. 1, pp. 90–102, 2008.
- [27] N. Yaghobi and M. H. R. Ghoreishy, “Oxidative coupling of methane in a fixed bed reactor over perovskite catalyst: A simulation study using experimental kinetic model,” *J. Nat. Gas Chem.*, vol. 17, no. 1, pp. 8–16, 2008.
- [28] M. Daneshpayeh, A. Khodadadi, N. Mostoufi, Y. Mortazavi, R. Sotudeh-Gharebagh, and A. Talebizadeh, “Kinetic modeling of oxidative coupling of methane over Mn/Na₂WO₄/SiO₂ catalyst,” *Fuel Process. Technol.*, vol. 90, no. 3, pp. 403–410, 2009.
- [29] K. Takanabe and E. Iglesia, “Mechanistic aspects and reaction pathways for oxidative coupling of methane on Mn/Na₂WO₄/SiO₂ catalysts,” *J. Phys. Chem. C*, vol. 113, no. 23, pp. 10131–10145, 2009.
- [30] Z. Taheri, N. Seyed-Matin, A. A. Safekordi, K. Nazari, and S. Z. Pashne, “A comparative kinetic study on the oxidative coupling of methane over LSCF perovskite-type catalyst,” *Appl. Catal. A Gen.*, vol. 354, no. 1–2, pp. 143–152, 2009.
- [31] N. Razmi Farooji, A. Vatani, and S. Mokhtari, “Kinetic simulation of oxidative

- coupling of methane over perovskite catalyst by genetic algorithm: Mechanistic aspects,” *J. Nat. Gas Chem.*, vol. 19, no. 4, pp. 385–392, 2010.
- [32] A. Farsi, S. Ghader, A. Moradi, S. S. Mansouri, and V. Shadravan, “A simple kinetic model for oxidative coupling of methane over $\text{La}_{0.6}\text{Sr}_{0.4}\text{Co}_{0.8}\text{Fe}_{0.2}\text{O}_{3-\delta}$ nanocatalyst,” *J. Nat. Gas Chem.*, vol. 20, no. 3, pp. 325–333, 2011.
- [33] V. I. Lomonosov, Y. A. Gordienko, and M. Y. Sinev, “Kinetics of the oxidative coupling of methane in the presence of model catalysts,” *Kinet. Catal.*, vol. 54, no. 4, pp. 451–462, 2013.
- [34] A. Valadkhani, M. Shahrokhi, M. R. Pishvaie, and S. Zarrinpashneh, “Simulation and experimental studies of methane oxidative coupling reaction in a bench scale fixed bed reactor,” *Energy Sources, Part A Recover. Util. Environ. Eff.*, vol. 35, no. 15, pp. 1418–1426, 2013.
- [35] J. Sadeghzadeh Ahari, S. Zarrinpashne, and M. T. Sadeghi, “Micro-kinetic modeling of OCM reactions over $\text{Mn}/\text{Na}_2\text{WO}_4/\text{SiO}_2$ catalyst,” *Fuel Process. Technol.*, vol. 115, pp. 79–87, 2013.
- [36] A. Vatani, E. Jabbari, M. Askarieh, and M. A. Torangi, “Kinetic modeling of oxidative coupling of methane over Li/MgO catalyst by genetic algorithm,” *J. Nat. Gas Sci. Eng.*, vol. 20, pp. 347–356, 2014.
- [37] D. Li, W. S. Baslyman, B. Siritanaratkul, T. Shinagawa, S. M. Sarathy, and K. Takanaabe, “Oxidative-Coupling-Assisted Methane Aromatization: A Simulation Study,” *Ind. Eng. Chem. Res.*, vol. 58, no. 51, pp. 22884–22892, 2019.
- [38] A. M. Dean, “Detailed kinetic modeling of autocatalysis in methane pyrolysis,” *J.*

- Phys. Chem.*, vol. 94, no. 4, pp. 1432–1439, 1990.
- [39] O. Rival, B. P. A. Grandjean, C. Guy, A. Sayari, and F. Larachi, “Oxygen-free methane aromatization in a catalytic membrane reactor,” *Ind. Eng. Chem. Res.*, vol. 40, no. 10, pp. 2212–2219, 2001.
- [40] L. Li, R. W. Borry, and E. Iglesia, “Reaction-transport simulations of non-oxidative methane conversion with continuous hydrogen removal - homogeneous-heterogeneous reaction pathways,” *Chem. Eng. Sci.*, vol. 56, no. 5, pp. 1869–1881, 2001.
- [41] L. Li, R. W. Borry, and E. Iglesia, “Design and optimization of catalysts and membrane reactors for the non-oxidative conversion of methane,” *Chem. Eng. Sci.*, vol. 57, no. 21, pp. 4595–4604, 2002.
- [42] M. C. Iliuta, I. Iliuta, B. P. A. Grandjean, and F. Larachi, “Kinetics of methane nonoxidative aromatization over Ru-Mo/HZSM-5 catalyst,” *Ind. Eng. Chem. Res.*, vol. 42, no. 14, pp. 3203–3209, Jul. 2003.
- [43] B. Yao, J. Chen, D. Liu, and D. Fang, “Intrinsic kinetics of methane aromatization under non-oxidative conditions over modified Mo/HZSM-5 catalysts,” *J. Nat. Gas Chem.*, vol. 17, no. 1, pp. 64–68, 2008.
- [44] K. S. Wong, J. W. Thybaut, E. Tangstad, M. W. Stöcker, and G. B. Marin, “Methane aromatisation based upon elementary steps: Kinetic and catalyst descriptors,” *Microporous Mesoporous Mater.*, vol. 164, pp. 302–312, 2012.
- [45] C. Karakaya, H. Zhu, and R. J. Kee, “Kinetic modeling of methane dehydroaromatization chemistry on Mo/Zeolite catalysts in packed-bed reactors,”

- Chem. Eng. Sci.*, vol. 123, pp. 474–486, 2015.
- [46] C. Karakaya, S. H. Morejudo, H. Zhu, and R. J. Kee, “Catalytic Chemistry for Methane Dehydroaromatization (MDA) on a Bifunctional Mo/HZSM-5 Catalyst in a Packed Bed,” *Ind. Eng. Chem. Res.*, vol. 55, no. 37, pp. 9895–9906, 2016.
- [47] N. I. Fayzullaev, “Kinetics and Mechanism of the Reaction of Catalytic Dehydroaromatization of Methane,” *Int. J. Oil, Gas Coal Eng.*, vol. 5, no. 6, p. 124, 2017.
- [48] Y. Zhu, N. Al-ebbinni, R. Henney, C. Yi, and R. Barat, “Extension to multiple temperatures of a three-reaction global kinetic model for methane dehydroaromatization,” *Chem. Eng. Sci.*, vol. 177, pp. 132–138, 2018.
- [49] J. Jeong, A. Hwang, Y. T. Kim, D. Y. Hong, and M. J. Park, “Kinetic modeling of methane dehydroaromatization over a Mo₂C/H-ZSM5 catalyst: Different deactivation behaviors of the Mo₂C and H-ZSM5 sites,” *Catal. Today*, vol. 352, no. June 2019, pp. 140–147, 2020.
- [50] W. Y. Tung and L. L. Lobban, “Oxidative Coupling of Methane over Li/MgO: Kinetics and Mechanisms,” *Ind. Eng. Chem. Res.*, vol. 31, no. 7, pp. 1621–1625, 1992.
- [51] Y. K. Kao, L. Lei, and Y. S. Lin, “A Comparative Simulation Study on Oxidative Coupling of Methane in Fixed-Bed and Membrane Reactors,” *Ind. Eng. Chem. Res.*, vol. 36, no. 9, pp. 3583–3593, 1997.
- [52] F. Bre, J. M. Gimenez, and V. D. Fachinotti, “Prediction of wind pressure coefficients on building surfaces using artificial neural networks,” *Energy Build.*,

- vol. 158, no. April 2018, pp. 1429–1441, 2018.
- [53] F. M. Dautzenberg, J. C. Schlatter, J. M. Fox, J. R. Rostrup-Nielsen, and L. J. Christiansen, “Catalyst and reactor requirements for the oxidative coupling of methane,” *Catal. Today*, vol. 13, no. 4, pp. 503–509, 1992.
- [54] A. P. de Wasch and G. F. Froment, “Heat transfer in packed beds,” *Chem. Eng. Sci.*, vol. 27, no. 3, pp. 567–576, Mar. 1972.
- [55] V. V. Kuznetsov, O. V. Vitovsky, S. V. Dimov, S. A. Safonov, and S. P. Kozlov, “Hydrodynamics and heat and mass transfer at chemical conversions in slot reactors,” *J. Eng. Thermophys.*, vol. 16, no. 2, pp. 99–106, 2007.
- [56] M. Leva, “Packed-Tube Heat Transfer,” *Ind. Eng. Chem.*, vol. 42, no. 12, pp. 2498–2501, Dec. 1950.
- [57] A. G. Dixon and D. L. Cresswell, “Theoretical prediction of effective heat transfer parameters in packed beds,” *AIChE J.*, vol. 25, no. 4, pp. 663–676, 1979.
- [58] E. Tsotsas and E. U. Schlünder, “Heat transfer in packed beds with fluid flow: remarks on the meaning and the calculation of a heat transfer coefficient at the wall,” *Chem. Eng. Sci.*, vol. 45, no. 4, pp. 819–837, 1990.
- [59] W. Wang and Y. S. Lin, “Analysis of oxidative coupling of methane in dense oxide membrane reactors,” *J. Memb. Sci.*, vol. 103, no. 3, pp. 219–233, Jul. 1995.
- [60] J. Jeong, A. Hwang, Y. T. Kim, D. Y. Hong, and M. J. Park, “Kinetic modeling of methane dehydroaromatization over a Mo₂C/H-ZSM5 catalyst: Different deactivation behaviors of the Mo₂C and H-ZSM5 sites,” *Catal. Today*, vol. 352, no. September 2019, pp. 140–147, 2020.

Appendix A

Efforts to reproduce kinetic models in literature

Although this section is not linked to my thesis, however, during reproducing kinetic models a lot of challenges were faced and it is thought to be valuable to be include it as information. During such studies of reactor modeling, six OCM kinetic models [36],[21],[28],[31],[32],[59] and four MDA kinetic models [42], [47][48], [60] were tried to be reproduced. This was a challenging process and various factors contribute towards making this process difficult, as mentioned below:

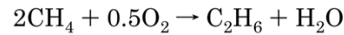
1. Missing information about design parameters:

This includes missing parameters like inlet compositions, feed ratio, flowrates, catalyst weight, GHSV and void fractions. These parameters are required for unit consistency of kinetic constants with the given reactor design equation and are needed for reactor modeling. For example, a kinetic parameter, k , is given in terms of catalyst weight (units $\text{gmol/g.cat.h.bar}^2$); whereas, if the design equation is in terms of reactor length, catalyst density and bed void fraction is required, which is usually missing.

2. Typing errors and missing definition of kinetic parameters:

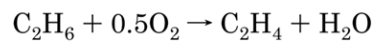
A kinetic expression represents the performance of a catalyst and any mistake or missing information can lead to wrong results. Hence, careful consideration is required while writing such expressions. As, for someone studying the model for the first time might not be able to make any proper judgements of the error.

Given below is an example of a commonly used OCM model[21], of which the delta enthalpy of adsorption and the partial pressure should have been of carbon dioxide but was reported that of oxygen:



$$r_2 = \frac{k_{0,2} e^{-E_{a,2}/RT} (K_{\text{O}_2} e^{-\Delta H_{\text{ad},\text{O}_2}/RT} p_{\text{O}_2})^{n_2} p_{\text{CH}_4}}{[1 + (K_{\text{O}_2} e^{-\Delta H_{\text{ad},\text{O}_2}/RT} p_{\text{O}_2})^n + \underline{K_{j,\text{CO}_2}} e^{\Delta H_{\text{ad},\text{O}_2}/RT} p_{\text{O}_2}^2]} \quad \text{VI.1}$$

An example of missing information can be understood from the following example[21]:



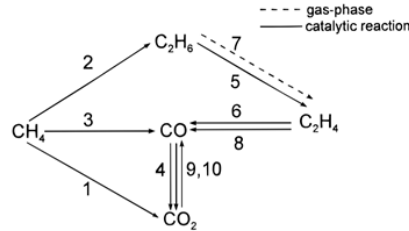
$$r_j = \frac{k_{0,j} e^{-E_{a,j}/RT} p_{\text{C}}^{m_j} p_{\text{O}_2}^{n_j}}{(1 + K_{j,\text{CO}_2} e^{-\Delta H_{\text{ad},\text{CO}_2,j}/RT} p_{\text{CO}_2})^n} \quad \text{VI.2}$$

Hereby, p_{C} is mentioned, which can be understood as the partial pressure of carbon. However, for the given reaction, there are components in the reactants as well as the products that contain carbon and can be quite challenging to understand which it is referring to.

3. Incomplete kinetic expressions:

A complete kinetic expression needs to have a rate of reaction represented with the reaction number and with respect to a particular component of the reaction. Some kinetic models are presented either with the reaction number or with the component only. This creates a challenge while incorporating into the design equation based on which stoichiometric coefficient to use.

Below is an example[21] where the kinetic expressions lack based on which component they are represented.



- step 1: $\text{CH}_4 + 2\text{O}_2 \rightarrow \text{CO}_2 + 2\text{H}_2\text{O}$
- step 2: $2\text{CH}_4 + 0.5\text{O}_2 \rightarrow \text{C}_2\text{H}_6 + \text{H}_2\text{O}$
- step 3: $\text{CH}_4 + \text{O}_2 \rightarrow \text{CO} + \text{H}_2\text{O} + \text{H}_2$
- step 4: $\text{CO} + 0.5\text{O}_2 \rightarrow \text{CO}_2$
- step 5: $\text{C}_2\text{H}_6 + 0.5\text{O}_2 \rightarrow \text{C}_2\text{H}_4 + \text{H}_2\text{O}$
- step 6: $\text{C}_2\text{H}_4 + 2\text{O}_2 \rightarrow 2\text{CO} + 2\text{H}_2\text{O}$
- step 7: $\text{C}_2\text{H}_6 \rightarrow \text{C}_2\text{H}_4 + \text{H}_2$
- step 8: $\text{C}_2\text{H}_4 + 2\text{H}_2\text{O} \rightarrow 2\text{CO} + 4\text{H}_2$
- step 9: $\text{CO} + \text{H}_2\text{O} \rightarrow \text{CO}_2 + \text{H}_2$
- step 10: $\text{CO}_2 + \text{H}_2 \rightarrow \text{CO} + \text{H}_2\text{O}$

$$r_2 = \frac{k_{0,2} e^{-E_{a,2}/RT} (K_{0,\text{O}_2} e^{-\Delta H_{\text{ad},\text{O}_2}/RT} p_{\text{O}_2})^{n_2} p_{\text{CH}_4}}{[1 + (K_{0,\text{O}_2} e^{-\Delta H_{\text{ad},\text{O}_2}/RT} p_{\text{O}_2})^n + K_{j,\text{CO}_2} e^{-\Delta H_{\text{ad},\text{O}_2,j}/RT} p_{\text{O}_2}]^2}$$

$$r_j = \frac{k_{0,j} e^{-E_{a,j}/RT} p_{\text{C}}^{m_j} p_{\text{O}_2}^{n_j}}{(1 + K_{j,\text{CO}_2} e^{-\Delta H_{\text{ad},\text{CO}_2,j}/RT} p_{\text{CO}_2})^n} \quad j = 1, 3-6$$

$$r_7 = k_{0,7} e^{-E_{a,7}/RT} p_{\text{C}_2\text{H}_6}$$

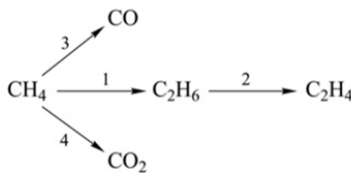
$$r_8 = k_{0,8} e^{-E_{a,8}/RT} p_{\text{C}_2\text{H}_4}^{m_8} p_{\text{H}_2\text{O}}^{n_8}$$

$$r_9 = k_{0,9} e^{-E_{a,9}/RT} p_{\text{CO}}^{m_9} p_{\text{H}_2\text{O}}^{n_9}$$

$$r_{10} = k_{0,10} e^{-E_{a,10}/RT} p_{\text{CO}_2}^{m_{10}} p_{\text{H}_2}^{n_{10}}$$

VI.3

Another example[32] where the kinetic expressions are represented in terms of the components, but not on the reactions:



- step 1: $2\text{CH}_4 + 0.5\text{O}_2 \rightarrow \text{C}_2\text{H}_6 + \text{H}_2\text{O}$
- step 2: $\text{C}_2\text{H}_6 + 0.5\text{O}_2 \rightarrow \text{C}_2\text{H}_4 + \text{H}_2\text{O}$
- step 3: $\text{CH}_4 + 1.5\text{O}_2 \rightarrow \text{CO} + 2\text{H}_2\text{O}$
- step 4: $\text{CH}_4 + 2\text{O}_2 \rightarrow \text{CO}_2 + 2\text{H}_2\text{O}$

$$R_{\text{CH}_4} = 5.375443 e^{-\frac{1049527}{RT}} P_{\text{CH}_4}^{0.39563} P_{\text{O}_2}^{0.72761}$$

$$R_{\text{C}_2\text{H}_4} = 0.108777366 e^{-\frac{833277.7}{RT}} P_{\text{CH}_4}^{0.6541} P_{\text{O}_2}^{0.618}$$

$$R_{\text{CO}_x} = 5.375443 e^{-\frac{1049527}{RT}} P_{\text{CH}_4}^{0.39563} P_{\text{O}_2}^{0.72761} - 0.217554732 e^{-\frac{833277.7}{RT}} P_{\text{CH}_4}^{0.6541} P_{\text{O}_2}^{0.618}$$

$$R_{\text{CO}_x} = R_{\text{CH}_4} - 2R_{\text{C}_2\text{H}_4}$$

VI.4

4. Unavailability of readily usable experimental data:

Since experimental data is not present in a tabular form but in the form of graphs. Thus, extraction is required from graphs for the purpose kinetic model validation. This can be very time consuming and also requires expertise on softwares that allow such features.

5. Missing definitions of reactor performance indicators

Results are usually mentioned in terms of reactor performance indicators like conversion, selectivity, and yield. However, these can be defined based on specific components and entirely depends on how the author uses it. However it is missing most of the time. Like selectivity of a component X; it can be defined as the amount of an X product produced with respect to the amount of the reactant consumed. However, it can also be defined as the amount of X product with respect to some specific products only, say D and E, and not product F. Whereas, someone else might define it with respect to products, D, E and F. Some of the different examples of how selectivity can be defined in multiple ways is below:

$$S_1 = \frac{2r_2}{2r_2 + 2r_{16}}$$

$$2R_{C_2}/(2R_{C_2} + R_{CO_2} + R_{CO})$$

$$S_{C_2H_4} \equiv 2F_{C_2H_4}/(F_{CH_4_0} - F_{CH_4})$$

$$S_{C_{2+}}(\%) = \frac{\sum(2 \times \text{moles of } C_{2+} \text{ in products})}{\text{Moles of } CH_4 \text{ converted to all products}} \times 100$$

$$S_{C\text{-products}}(\%) = \frac{\text{moles of carbon in the specific product}}{\text{total moles of carbon in products}} \times 100$$

$$S_{C_2H_4}\% = \frac{2 * \text{moles of } C_2H_4 \text{ in products}}{(\text{moles of } CO + \text{moles of } CO_2 + 2 * (\text{moles of } C_2H_4 + \text{moles of } C_2H_6) \text{ in products})} * 100$$

VI.5

6. Wrong or truncated axes used for result representation

Some results can be misleading due to wrong axial titles. For example [21], in the case given below, reactor performances with respect to GHSV is shown:

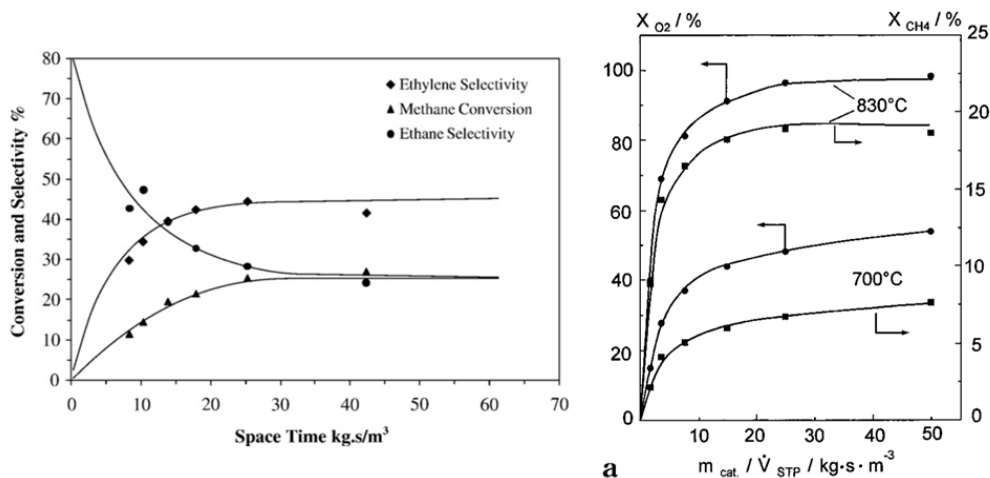


Figure VI.1 Graphical results of some kinetic models of OCM

Similar result for another kinetic models is shown below [36], however, the results contradict with the above two models because the axes are misrepresented as space velocity and not as space time.

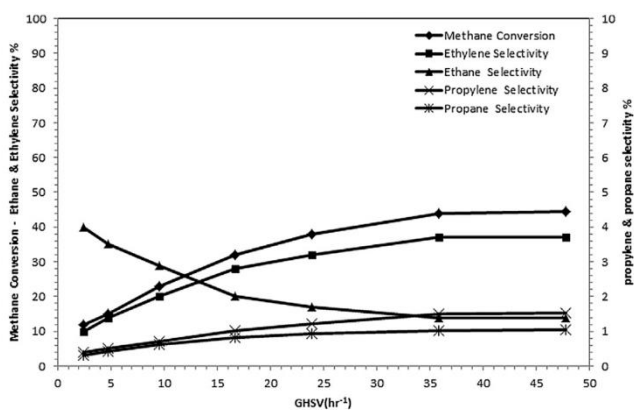


Figure VI.2 Graphical result of a kinetic model of OCM

Another challenge of graphical representation is truncated axes, which can make the results be unclear and misinterpreted. An example [51] is given below for which the y-axis on the right side of the graph that represents ethane mole fraction is truncated and hence the values cannot be understood:

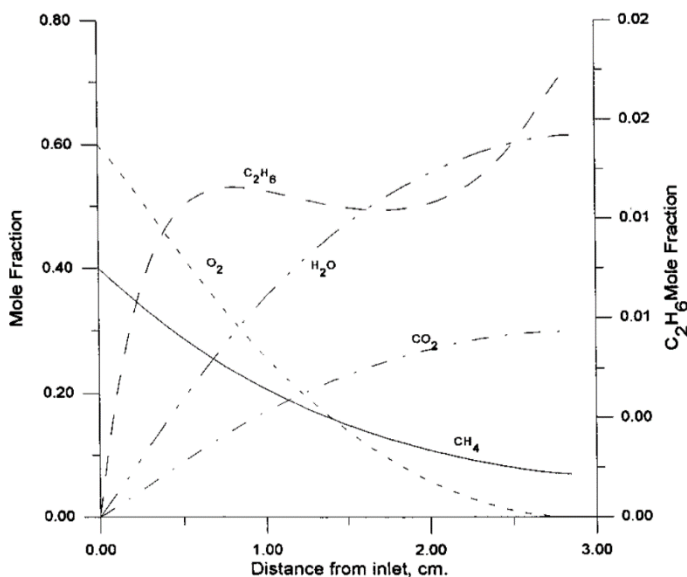


Figure VI.3 Graphical results of a kinetic model of OCM

7. Missing or different statistical tests for kinetic model's accuracy

Different statistical tests are used to represent a kinetic model's accuracy like Mean Average Relative Error, Average Absolute Relative Deviation, Percent of Square Deviation, R squared etc. However, while comparing one model with the other, such a variety of statistical results can be hard to compare, particularly when some models do not have any accuracy results.

8. Validation of models done for limited reaction conditions

Validation of the kinetic models is done to be able to work on those models and simulate further results. However, since validation of a kinetic model is quiet challenging and hence

some validations are specific to the conditions and not to the entire range of the model. This provides a false impression towards the kinetic model that it is reproducible, whereas, it may not be in reality.

9. Missing bulk catalyst bed density

The density is presented as that of the catalyst, and not bulk density i.e. it excludes the diluent. However, the results with respect to the catalyst bed length which includes the presence of the catalyst and the diluent. Hence the results can be deviating since conversion from the weight of catalyst to the bed length requires the density of the whole bed and not only the catalyst.